UC Davis
UC Davis Electronic Theses and Dissertations

Title

A Review of Drivers for Implementing Geopolymers in Construction: Codes and Constructability

Permalink

https://escholarship.org/uc/item/9kf0f1dv

Author

Martinez, Andres

Publication Date

2024

Peer reviewed|Thesis/dissertation

eScholarship.org Powered by the California Digital Library
University of California

A Review of Drivers for Implementing Geopolymers in Construction: Codes and Constructability

By

ANDRES MARTINEZ

THESIS

Submitted in partial satisfaction of the requirements for the degree of

MASTER OF SCIENCE

in

ENERGY SYSTEMS

in the

OFFICE OF GRADUATE STUDIES

of the

UNIVERSITY OF CALIFORNIA

DAVIS

Approved:

Sabbie A. Miller, Chair

Alissa Kendall

Somayeh Nassiri

Committee in Charge

2024

© Andrés I. Martínez, 2024. All rights reserved.

Content reproduced with permission from the original publisher, Elsevier B.V.

To all those who pursue their dreams with determination.

Contents

Abstract

Geopolymer concrete (GPC) has emerged as an alternative to Portland cement (PC) concrete in recent decades, with recent drivers for its use being tied to its potential environmental sustainability benefits and comparable performance. However, many aspects influencing its implementation are yet to be fully addressed. This work presents a systematic review of the literature to address unique drivers in the material performance of GPC and the role of current standardization methods in utilizing this class of materials in construction practice. The review highlights common GPC constituents and addresses how variations in the properties or proportioning of these constituents influence GPC performance characteristics and constructability. Notably, the performance of GPC is shown to be highly influenced by mixture parameters across many mechanical, durability, and constructability metrics, a key consideration for the application of this class of materials. Further, standardized test methods for GPC in selected regions are addressed, and the suitability of testing procedures outlined in the American Concrete Institute (ACI), ASTM International, the International Organization for Standardization (ISO) and other relevant specifications for assessing GPC is presented. The findings of this review highlight the need for developing non-prescriptive testing procedures for GPC and the adoption of specifications that have flexibility for alternatives to conventional PC concrete.

Acknowledgments

Throughout this journey, I was immensely fortunate to receive the support and encouragement of many individuals who contributed to my development as a scholar and as a person. Words cannot express my gratitude to them.

Firstly, I would like to extend my deepest appreciation to my advisor, Professor Sabbie A. Miller. Without her guidance, support and resourcefulness, I would not have been able to achieve any of my graduate school goals. Her exceptional work ethic and insightful feedback and advice have all influenced and shaped how I approach my own work. Additionally, I want to thank Professor Miller for her patience and understanding, especially when I was not feeling well physically or mentally. Her care for our mental health and well-being is much appreciated. I could not have wished for a better advisor and role model.

I am also thankful to Professors Alissa Kendall and Somayeh Nassiri for reviewing my manuscript and helping me improve it. Special thanks to Professor Kendall, whose mentoring and advice facilitated my graduate school experience and helped me take the following steps in my career. My gratitude also goes to Priya and Jim, my project managers at Google, who gave me valuable feedback on my projects and happily supported my education. I appreciate your commitment to improving the building industry and supporting climate change research.

I cannot leave out my colleagues from the Energy Graduate Group and the Green Engineered Materials and Systems group, who have greatly enriched me with their points of view on energy systems and sustainability. I want to thank you all for our good times together in Davis.

Lastly, I would like to extend my heartfelt thanks to my family and friends in California and Panama. Your unwavering support and encouragement have been my anchor

throughout this journey. Your belief in me, even during the most challenging times, has been a constant source of strength. I am truly blessed to have you in my life.

Chapter 1

Introduction

1.1. Background

Over the last decade, the adoption of sustainable development goals has prompted the building industry to pursue climate change mitigation strategies. However, these shifts towards mitigating environmental impacts have had to be addressed while still responding to the growing demands for construction worldwide (Swilling et al., 2018). Notably, approximately 1 billion more people are projected to move to urban areas by 2030, increasing the demand for new infrastructure and requiring the upgrade of aging systems (Olsson et al., 2023).

One of the main concerns for the construction sector is the massive amount of greenhouse gas (GHG) emissions associated with materials production. In this regard, one of the most substantial sources of building materials-related GHG emissions is the manufacturing of Portland cement (PC), the traditional binding agent in concrete. Manufacturing PC-based materials, such as concrete, accounts for an estimated 8% of global anthropogenic CO_2 emissions and 2–3% of energy use (Monteiro et al., 2017). The primary processes responsible for these GHG emissions are the decarbonation of limestone (calcination) and the use of high-emitting fuels in kilns operated at high temperatures (∼1450 °C) to obtain clinker, the main component of PC. The notable scale of these emissions is a function of the high global demand for PC. In addition to CO_2 emissions, the high demand for PC

globally also contributes to large water demand and to air pollutant emissions (Almutairi et al., 2021). During the last century, demand for PC has increased continuously, outpacing the population growth rate by a factor of ten, with current production exceeding 4 billion metric tons annually (Miller & Myers, 2019).

As the need to reduce the GHG emissions from the cement industry becomes more evident and urgent, many emissions mitigation strategies have been proposed in the literature. Such strategies have included energy efficiency techniques, the use of alternative fuels for the rotary kilns, the implementation of carbon capture and storage technologies, and replacing PC with sustainable low-carbon alternatives (Busch et al., 2022; Habert et al., 2020). Alternative cements have gained popularity over the last decade due to their environmental benefits, lower energy demand and satisfactory performance (Pacheco-Torgal et al., 2015). Among the most promising substitutes for PC are alkali-activated materials (AAMs). These binders are made from aluminosilicate solid precursors and alkaline solutions. The most common activators and precursors for manufacturing AAMs include (Shi et al., 2006):

- Alkaline activators: sodium hydroxide, sodium silicate, sodium carbonate, potassium hydroxide, and potassium silicate.
- Aluminosilicate precursors: coal fly ash, granulated blast furnace slag, granulated phosphorus slag, steel slag, non-ferrous slag, metakaolin, silica fume, volcanic glasses, and zeolite.

An alkaline activator can activate the precursor compounds to form a highly cross-linked network, creating a hardened matrix. Among the most prevalent AAMs are low-calcium AAMs, referred to as geopolymer binders (Provis, 2018). Due to the prevalence of geopolymer binders in the literature, geopolymer and AAM are used interchangeably herein. AAMs can bind together fine aggregates, fillers, and coarse aggregates, not unlike PC concrete, to form a concrete alternative, which is referred to herein as geopolymer concrete (GPC).

The potential environmental sustainability of these alternative binders and concretes is a function of several factors. Among the most used aluminosilicate solid precursors are by-products from other industries (e.g., fly ash, from coal-fired electricity generation; slag, from the iron and steel refining industry). Using such by-products and the ability to form a binding system without calcination and kilning can reduce GHG emissions by 80% compared to PC, depending on the AAM composition (Tayeh et al., 2021). Other reported benefits of AAM binders include improving the circular economy through waste valorization, highly tunable mechanical performance, resistance to certain chemical deterioration mechanisms, desirable thermal properties (e.g., high fire resistance), notable durability under freeze and thaw cycles, exceptionally low air and water permeability, and longer service life (Almutairi et al., 2021; Hassan et al., 2019b).

Despite key desirable characteristics and robust technical knowledge of GPC, the deployment and adoption of these materials as a replacement for conventional PC-based concrete still face challenges. Key barriers include control of the supply chain, reliance on alkali suppliers, lack of adequate training for some technologies, and lack of performance-based standards (Almutairi et al., 2021; Provis, 2018). Also, higher production costs compared to PC, elevated workability loss rate, quick setting times, and need for heat curing are among other concerns for industry stakeholders.

1.2. Contributions

This work synthesizes the literature to explore parameters that have been highlighted as key drivers to limiting the implementation of GPC. Among these are: (a) persistent concerns of differences in material performance relative to PC concrete; (b) concerns of differences in placing the material and shifts in constructability that may warrant education of construction workers; (c) concerns regarding the ability to meet code requirements; and (d) concerns in differences in appearance or aesthetics of GPC relative to PC concrete.

To address these concerns, this literature review uniquely focuses on encompassing material behavior from fresh properties, mechanical performance, and durability through code development and barriers to constructability and adoption. Findings provide critical insights into measures that could drive GPC utilization and inform key stakeholders throughout the supply chain of the applicability of this class of materials for construction projects. Namely, this research provides a 1) summary of resources used in geopolymer binders and their impact on fresh and hardened concrete properties and 2) a review of the existing standards and codes that apply to geopolymer binders and concrete.

The subsequent sections focus on describing components of geopolymer binders (Chapter 2), drivers for change in material behavior, shifts in workability and constructability of GPC relative to PC concrete, the role of pigmentation in altering material behavior (Chapters 3 to 5), and the state of codes and standards, as well as factors that have facilitated the use of GPC that meets standards (Chapter 6). The findings from this review contextualize barriers to using GPC in conventional construction and highlight pathways to overcome such barriers. Further, areas that require additional research to support geopolymer implementation are identified. Details on the research methodology can be found in the Appendix A.

The content presented throughout this work appears in:

> Martínez, A., & Miller, S. A. (2023). A review of drivers for implementing geopolymers in construction: Codes and constructability. Resources, Conservation and Recycling, 199, 107238. doi: https://doi.org/10.1016/j.resconrec.2023.107238

Chapter 2

Alkaline Activators and Geopolymer Binders

2.1. Types of alkali-activated systems

Over the past few decades, various types of AAMs have been developed. These AAMs can be classified into three main categories according to the nature of their cementitious components (Nodehi & Taghvaee, 2022; Pacheco-Torgal et al., 2015):

- Low calcium-based systems: these compounds primarily utilize materials rich in aluminosilicates with a relatively low calcium content (e.g., metakaolin or Class-F fly ash). The final reaction product is a three-dimensional inorganic N-A-S-H gel (sodium aluminosilicate hydrate), which exhibits a long setting time and requires thermal curing to develop strength. However, it offers advantages such as elevated fire resistance, low permeability and high chloride and carbonation resistance. As noted previously, low-calcium systems are often referred to as geopolymer binders.
- High calcium-based systems: they comprise aluminosilicate precursors with high calcium oxide content, such as ground granulated blast furnace slag and Class-C fly ash. High-calcium systems are used in a relatively moderate alkaline condition, forming calcium aluminosilicate hydrate (C-A-S-H) gel. The higher level of calcium leads to faster hardening, lower setting time, and higher early strength.

- Blended or hybrid systems: this model combines PC clinker and AAM-binders. The main reaction products are low and high calcium systems, i.e., a blend of N-A-S-H and C-A-S-H gels. This review focuses on low and high-calcium AAMs and not hybrid cement systems.

2.2. Aluminosilicate precursors

The purpose of aluminosilicate precursors in AAMs is to provide a source of reactive components that alkali solutions can easily activate. Since the invention of AAMs, many precursors have been investigated. Based on the academic literature, this study explores 17 commonly reported solid precursors that are utilized in the manufacturing of AAMs and GPC (Almutairi et al., 2021; Shah et al., 2022; García-Lodeiro et al., 2015; Shi et al., 2006; Nodehi & Taghvaee, 2022; Assi et al., 2020; Shehata et al., 2022):

- Low-calcium fly ash (Class-F fly ash): Class-F fly ash is a by-product of coal-fired electricity generation. It is captured using electrostatic precipitators or fabric collectors during pulverized anthracite or bituminous coal combustion in furnaces at 1500 ± 200 °C.
- High-calcium fly ash (Class-C fly ash): Similar to Class-F fly ash, Class-C fly ash is a by-product of coal-fired electricity generation. However, it is captured during the calcination of lignite or sub-bituminous coal.
- Ground-granulated blast furnace slag (GGBFS): GGBFS is a by-product of pig iron production in blast furnaces at 1500 ± 100 °C. The acid gangue in iron ore combines with coke sulfur, lime and magnesium to form the slag, which is subsequently tapped off, quenched in water, dried and grounded to a fine powder.
- Metakaolin (MK): MK is obtained by heating kaolinite (a clay mineral) until it becomes fully dehydrated and its atomic structure is destroyed (dehydroxylation). MK with high pozzolanic reactivity is typically produced between 600 and 900 °C.

- Silica fume (SF): SF is a by-product of silicon and ferrosilicon alloy manufacturing. It is obtained by reducing the quartz to silicon at ∼2000 °C in induction arc furnaces.
- Rice husk ash (RHA): RHA is a bio-derived waste from burning rice husk to generate electricity. RHA contains reactive amorphous silica that can be used as a pozzolan material.
- Red mud (RM): Bauxite residue, or red mud (RM), is a mineral tailing and by-product that originates during the alumina extraction from bauxite ores using the Bayer process.
- Waste glass (WG): WG is a recyclable waste that exhibits pozzolanic properties that allow its use as a precursor (in the form of powder). It is generated from industrial processes and human activities.
- Natural zeolites (NZ): NZ are microporous pozzolanic hydrated crystalline aluminosilicate structures created from the crystallization of ash and rock layers. There are approximately 45 types of NZ, with clinoptilolite and mordenite being among the most extensively used in industrial applications.
- Basalt (BA): BA is a dark-colored igneous rock with low reactivity. It is formed from the solidification of lava flows, making it one of the most common rock types on Earth's crust.
- Bamboo leaf ash (BLA): BLA is pozzolanic material obtained by calcinating bamboo leaves in electric arc furnaces at 600 °C for ∼2 h.
- Rice straw ash (RSA): The combustion of rice straw, a crop residue of rice harvesting, produces RSA, which exhibits pozzolanic behavior.
- Olive waste ash (OWA): OWA originates from solid waste combustion from olive oil production. The olive mill waste is burned in ovens at 800 °C for 8 h and then finely grounded for 3 h.

- Palm oil fuel ash (POFA): POFA is a by-product of the palm oil industry. It is obtained during the combustion of empty fruit bunches and nutshells from crude palm oil to generate electricity in palm oil factories.
- Mine tailings (MT): MT are a mixture of small stone fragments and waste materials generated by mining operations to extract valuable minerals and metals from ore. These tailings are produced by ore beneficiation, where over 50% of the total volume of ore is transformed into tailings. Note, due to the breadth of composition possible, only some MT would have an appropriate composition for use in AAMs.
- Silico-manganese slag (SiMnS): SiMnS is a by-product created during the production of silicomanganese (SiMn), a specific type of ferroalloy used to enhance the mechanical properties of steel. SiMn alloy is produced by reducing raw materials using carbothermic reactions in a submerged arc furnace at 1600 °C.
- Granulated phosphorus slag (GPS): GPS is a by-product generated in electric furnaces during the manufacture of yellow phosphorus. This industrial residue poses significant environmental problems and requires a considerable amount of space for storage.

Table 2.1 summarizes the availability, benefits, and limitations of these 17 potential solid precursor sources. As noted in this table, many of these solid precursors are by-products or residues derived from human activities. Their implementation not only contributes to the building industry sustainability (as alternatives to clinkered materials), but also promotes product recycling and prevents massive landfill disposals. For example, the study by Vincevica-Gaile et al. (2021) discusses the use of secondary raw materials (by-products) as an alternative to conventional methods for soil stabilization in peatlands, including ashes from agriculture, energy generation, and manufacturing processes. Notably, the authors highlight the use of geopolymers and by-products to abate GHG emissions, reduce the demand for virgin materials and promote waste valorization. Furthermore, the physiochemical characteristics of the solid precursors used in GPC are among the

primary drivers in the GPC material performance achieved. While many factors of these precursors affect the final behavior of the GPC, among the primary drivers are the composition, particularly the presence of Ca content and reactive Si and/or Al compounds that can contribute to the binding gel. Additionally, the amorphous content of the precursors can strongly affect reactivity, where a greater degree of amorphous content can facilitate improved reactivity of materials. Reactivity can also be driven by factors such as particle size and porosity. These characteristics of the precursor are driven by several parameters, including the primary source of the precursor (e.g., type of industrial waste), processing conditions that resulted in the precursor formation (e.g., the temperature at which the resource was formed), and post-formation processing (e.g., grinding to increase surface area to volume ratios). We summarize some of the key physiochemical characteristics of commonly discussed solid precursors in Appendix Tables B.1 and B.2.

Table 2.1: Summary of the aluminosilicate precursors found in the literature.

Aluminosilicate precursor	Production (Mt/year)	Benefits	Limitations	References
Industrial by-products				
Low-calcium fly ash (Class-F FA)	350-900 (globally available FA, 2018)	• Improved workability and slump rate, long-term mechanical properties and abrasion resistance. • Reduced air content and heat of hydration. • Reduced global warming potential relative to PC. • Reduced shrinkage and weathering influence compared to PC.	• Limited cementitious properties due to its low CaO content. • Low reactivity and early-age strength. • Increased setting time. • Exposure and transportation of fly ash can harm humans, animals and the environment.	Almutairi et al. (2021), Shah et al. (2022), García-Lodeiro et al. (2015), Shi et al. (2006), Nodehi and Taghvaee (2022), Assi et al. (2020), Miller et al. (2019).
High-calcium fly ash (Class-C FA)	350-900 (globally available FA, 2018)	• Good pozzolanic and cementitious properties. • Improved workability. • Reduced air content and water requirements. • Reduced chloride ingress. • High compressive strength (with heat curing). • Reduction in global warming potential relative to PC.	• Increased alkali-silica reaction potential • Not as widely available as Class-F fly ash, making it more costly.	Almutairi et al. (2021), Shah et al. (2022), García-Lodeiro et al. (2015), Miller et al. (2019).

Continued on next page

Table 2.1 – continued from previous page

Aluminosilicate precursor	**Production (Mt/year)**	**Benefits**	**Limitations**	**References**
Ground-granulated blast furnace slag (GGBFS)	300-360 (globally, 2018)	• Improved long-term strength. • Smooth compaction and placing due to enhanced workability. • High resistance to chloride ingress, sulfate attack, weathering and alkali-silica reaction. • Extended setting times (also depending on the temperature conditions). • Reduced risk of thermal cracking. • Sustainability advantages.	• Slower early strength development compared to PC. • Combined with MK, GGBFS-based GPC exhibits lower elastic modulus and higher shrinkage and porosity.	Shah et al. (2022), Shi et al. (2006), Nodehi and Taghvaee (2022), Suresh and Nagaraju (2015), Shehata et al. (2022), Almutairi et al. (2021), Souza et al. (2023).
Silica fume (SF)	1-3 (globally, 2018)	• High compressive strength and other mechanical properties. • Increased compaction. • Improved corrosion resistance. • Reduction in the cost and environmental impacts of GPC.	• Workability reduction. • Increased drying shrinkage. • High reactivity and limited quantities make this material typically expensive and prioritized for other applications.	Shah et al. (2022), Shi et al. (2006), Nodehi and Taghvaee (2022), Shehata et al. (2022).

Continued on next page

Table 2.1 – continued from previous page

Aluminosilicate precursor	**Production (Mt/year)**	**Benefits**	**Limitations**	**References**
Silico-manganese slag (SiMnS)	19.2-20.8 (globally, 2018)	• Acceptable compressive strength (with pre-treatment). • Accelerated setting time. • Environmental and economic benefits.	• Low reactivity compared to other cementitious materials. • Requires pre-treatment for geopolymerization (usually mechanical activation).	S. K. Nath et al. (2022), Marsh et al. (2021).
Granulated phosphorus slag (GPS)	>11.6 (U.S. and China, 2021)	• The addition of GPS reduces the setting time of fly ash-based GPC. • Improved compressive strength when added to fly ash-based GPC.	• GPC made with GPS requires heat curing for developing high early-age strength.	Wang et al. (2021).
Industrial wastes				
Waste glass (WG)	50-100 (globally, 2021)	• WG can improve the packing (in fine scales). • It can act as a filler or replace natural aggregates. • WG provides a supplementary silica source. • GPC made with WG can yield acceptable compressive strength under appropriate activator contents and curing conditions.	• Low hydration and integration. • Less reactive than other supplementary cementitious materials. • High expansion and alkali-silica reaction when used as an aggregate. • GPC made with WG requires additional sources of aluminum to stabilize.	Nodehi and Taghvaee (2022), Provis et al. (2015), Blengini et al. (2012).

Continued on next page

Table 2.1 – continued from previous page

Aluminosilicate precursor	Production (Mt/year)	Benefits	Limitations	References
Agricultural residues				
Rice husk ash (RHA)	100-200 (globally, 2021)	• Its high content of amorphous silica yields high reactivity. • Decreases shrinkage and bulk density. • Improves the microstructural packing. • Reduced environmental impacts (green material). • Low heat of hydration. • Enhanced durability.	• Requires a secondary source of alumina. • High percentages of RHA diminish compressive strength and workability. • Strong variability in mechanical properties and durability according to particle size and quality. • Increased setting time. • If inhaled, RHA can cause serious health issues.	Almutairi et al. (2021), Shah et al. (2022), Suresh and Nagaraju (2015), Nodehi and Taghvaee (2022), Miller et al. (2019), Shehata et al. (2022).
Bamboo leaf ash (BLA)	20 (globally)	• Improved durability (acid resistance and chloride resistance). • Low strength loss. • Environmental impact reduction relative to PC. • Cost reduction relative to PC (on a volume basis).	• Reduced compressive strength. • Increased water demand.	Thomas et al. (2021), Asha et al. (2014), Pereira et al. (2021).

Continued on next page

Table 2.1 – continued from previous page

Aluminosilicate precursor	**Production (Mt/year)**	**Benefits**	**Limitations**	**References**
Rice straw ash (RSA)	103-110	• RSA can produce marginal strength gains. • Environmentally friendly.	• The addition of RSA in concrete reduces workability. • The setting time and water demand increase with the content of RSA.	Thomas et al. (2021), El-Sayed and El-Samni (2006).
Olive waste ash (OWA)	∼4	• Enhanced workability. • OWA has high aluminum content which accelerates hydration. • Improved fire resistance. • Higher compressive strength relative to PC. • Good strength development.	• Increased water demand and porosity.	Thomas et al. (2021).
Palm oil fuel ash (POFA)	10 (Malaysia, 2011), 0.1 (Thailand)	• Improved compressive strength when blended with fly ash or GGBFS in GPC composites. • Lower drying shrinkage compared to PC. • Higher chloride and sulfate attack resistance relative to PC.	• High water demand. • If not properly ground, POFA can substantially reduce the compressive strength of concrete.	Provis et al. (2015), Khankhaje et al. (2016), Santhosh et al. (2022).
Mining residues				

Continued on next page

Table 2.1 – continued from previous page

Aluminosilicate precursor	**Production (Mt/year)**	**Benefits**	**Limitations**	**References**
Red mud (RM)	140-155	• Exhibits elevated alumina content that benefits geopolymerization. • RM already contains NaOH, thus reducing the NaOH solution demand for the activation process. • RM can improve compressive strength and setting time at low contents (5-20%). • Its use in GPC can help mitigate the economic and environmental issues associated with its disposal. • The addition of RM (up to 15% by weight) to fly ash-based GPC reduces the setting time.	• High alkalinity and impurities. • An increase in the RM content can expand the efflorescence area. • Reduced ductility. • RM disposal represents an environmental issue (arsenic emissions to water).	Almutairi et al. (2021), Shah et al. (2022), Provis et al. (2015), Nodehi and Taghvaee (2022), Kumar et al. (2021).

Continued on next page

Table 2.1 – continued from previous page

Aluminosilicate precursor	**Production (Mt/year)**	**Benefits**	**Limitations**	**References**
Mine tailings (MT)	5000-8000 (globally, 2014)	• The compressive and flexural strengths of GPC made with MT depend on the mineral employed. For example, copper-based GPC enhanced compressive strength under a certain amount of activator and curing conditions. • Using MT can reduce the environmental impact of concrete and reduce the amount of waste from mines.	• Low interaction during the geopolymerization reaction. • MT require pre-treatment to enhance the geopolymerization. • High drying shrinkage and efflorescence.	X. He et al. (2022), Qaidi et al. (2022).
Natural pozzolans				
Metakaolin (MK)	2.2-2.6 (globally, 2018)	• Better mechanical properties and microhardness. • Combined with coarse aggregates, they exhibit higher compressive strength (∼15% relative to PC).	• Workability reduction. • Higher shrinkage. • Low splitting tensile strength.	García-Lodeiro et al. (2015), Shi et al. (2006), Nodehi and Taghvaee (2022), Shehata et al. (2022).

Continued on next page

Table 2.1 – continued from previous page

Aluminosilicate precursor	**Production (Mt/year)**	**Benefits**	**Limitations**	**References**
Natural zeolites (NZ)	>>80 (globally, 2022)	• The addition of NZ can increase the compressive strength of concrete composites. • NZ can improve the chloride permeability of concrete.	• Reduction of workability. • Require high superplasticizer content. • High contents of NZ can increase the porosity of concrete abruptly. • NZ can lower the compressive strength if it is not carefully mixed.	Tran et al. (2019), Cherian et al. (2022).
Basalt (BA)	BA is the most common volcanic rock on the Earth's surface, and its global reserves are virtually inexhaustible.	• Improved hydration. • BA powder can reduce the void rate in concrete. • BA can improve compressive strength when used as a substitute for other aggregates.	• Low levels of aluminum. • Reduced workability.	Mao et al. (2022), Dobiszewska (2020).

2.3. Alkaline activators

Alkaline solutions play two important roles in the creation of an AAM binder: 1) dissolving the bonding between Si-O and Al-O and their following re-establishment in the matrix, and 2) balancing the mixture's charge using alkali-metal cations (Nodehi & Taghvaee, 2022). Further, the alkaline activators can be obtained in liquid or solid form to create alkaline solutions, influencing their cost and reactivity. Based on the academic literature, six commonly reported alkaline activators that are utilized in the manufacturing of AAMs and GPC are explored (Shi et al., 2006; Pacheco-Torgal et al., 2015; Nodehi & Taghvaee, 2022; García-Lodeiro et al., 2015):

- Sodium hydroxide (NaOH): Commonly known as caustic soda or lye, sodium hydroxide is a highly corrosive inorganic compound made of sodium cations and hydroxide anions. It is employed in various applications, such as manufacturing soap, paper, dye, detergent, and petroleum by-products. Commercially available NaOH is obtained through the chloralkali process.
- Sodium silicate ($(Na_2O)_x(SiO_2)_y$): Sodium silicate is the universal name of the chemical compounds formed with sodium oxide $[(Na_2O)_x]$ and silica $[(SiO_2)_y]$. The main sodium silicate used for alkaline activation is sodium metasilicate (Na_2SiO_3), produced by melting sand and sodium carbonate in furnaces at 1350–1400 °C. As explained later, sodium silicate and sodium hydroxide are commonly blended to obtain a compound activator, which can benefit GPC.
- Sodium carbonate (Na_2CO_3): Sodium carbonate, also known as soda ash, is an inorganic compound that can be obtained from natural sources and through manufacturing processes. Natural Na_2CO_3 is contained in several minerals, such as thermonatrite, trona, and nahcolite. Synthetic Na_2CO_3 can be obtained by the Solvay process or the ammonium chloride and caustic carbonation process. Typical applications of Na_2CO_3 include the manufacturing of glass, soap, paper, and detergents.

- Potassium hydroxide (KOH): Potassium hydroxide is another inorganic compound with several applications in the industry, such as manufacturing soaps and batteries. KOH is obtained through electrolysis of potassium chloride or by combining potassium carbonate and calcium hydroxide. It is characterized for being a strong base with high corrosiveness.
- Potassium silicate ($K_2O \cdot nSiO_2$): Similar to sodium silicate, potassium silicate is a general name encompassing a group of chemical compounds. Within this group, potassium metasilicate (K_2SiO_3) is the preferred solution used as an alkaline activator. It is obtained by synthesizing silica and potassium hydroxide or melting high-purity sand with potassium carbonate. (K_2SiO_3) is commonly used to fabricate cleaning agents, fertilizers and as a fire inhibitor for wood.
- Sodium sulfate (Na_2SO_4): Though less frequently discussed than other activators due to its lower alkalinity, sodium sulfate has also been employed for geopolymer binder manufacturing. This inorganic compound can be obtained from natural sources, such as brines and evaporites (e.g., thenardite, hanksite), or as a by-product of myriad chemical processes (e.g., viscose rayon production, hydrochloric acid synthetization). Among the common applications of Na_2SO_4 is the manufacturing of detergents, glass and paper.

Table 2.2 summarizes the availability, benefits, and limitations of these six alkaline solution sources. Additionally, Table B.3 in the Appendix synthesizes the key physical properties of the selected alkaline activators. As in the case of aluminosilicate precursors, the chemical features of the alkaline activators also play a crucial role in the geopolymerization process. For example, the silica modulus (SiO_2/N_2O) of sodium silicate solutions has a notable effect on the strength and microstructure of geopolymer binders. Lv et al. (2021) found that decreasing the silica modulus and increasing the dosage of sodium silicate enhanced the activation of fly ash, leading to GPC with superior microstructure and higher compressive strength. Further, these authors noted an ideal 10% wt. dosage

of sodium silicate when a high-modulus solution ($SiO_2/N_2O = 3.3$) was employed to activate fly ash-based GPC. The research by Firdous and Stephan (2019) also noted that reducing the silica modulus of sodium silicate improves the degree of reaction of natural pozzolans (i.e., precipitates more alumina and silica); nonetheless, lower silica modulus can also produce efflorescence, thus reducing compressive strength. Since high silica modulus also diminishes compressive strength, this approach requires determining the optimum silica modulus for the geopolymer mix. Notably, this optimum silica modulus is strongly influenced by the composition of aluminosilicate precursors, as observed by the authors.

Table 2.2: Summary of common alkaline activators used for GPC manufacturing.

Alkaline activator	Production (Mt/year)	Benefits	Limitations	References
Sodium hydroxide (NaOH)	72 (globally, 2016)	• When applied in combination with fly ash, it can improve the compressive strength of GPC. • NaOH can accelerate hydration. • High availability and lower costs ($770–920/ton in the U.S.).	• Highly corrosive (it can cause severe burns). • Viscosity increases with more concentration. • A decrease in strength usually occurs after 7 to 14 days of hydration. • Efflorescence.	Shi et al. (2006), Nodehi and Taghvaee (2022), Assi et al. (2020).
Sodium silicate (Na_2SiO_3)	12 (globally, 2020)	• Na_2SiO_3 is considered one of the most effective alkaline activators in the literature. • Na_2SiO_3 makes a dual contribution to the strength development of slag: as an alkaline activator and as an inducer of high-silica primary gel formation.	• Sodium silicate's properties are very sensitive to composition and storage conditions. • Na_2SiO_3 usually requires drying to reduce the moisture content during its manufacturing. • Substantial increase in viscosity is observed after 7% of Na_2O content.	Shi et al. (2006), Assi et al. (2020).

Continued on next page

Table 2.2 – continued from previous page

Alkaline activator	Production (Mt/year)	Benefits	Limitations	References
Sodium carbonate (Na_2CO_3)	58 (globally, 2022)	• Less costly than other alternatives due to its high availability. • Less corrosive than other activators. • Reduces the pH of the system. • More environmentally friendly than NaOH and Na_2SiO_3.	• Slow strength development and hardening compared to sodium hydroxide and sodium silicate-based systems.	Pacheco-Torgal et al. (2015), Shi et al. (2006), Adesina (2021).
Potassium hydroxide (KOH)	0.7-0.8 (globally, 2005)	• Lower porosity/dense microstructure. • KOH leaches aluminum and silicon at a higher rate than NaOH.	• Potassium-based activators are more costly than sodium-based activators. • Lower strength compared to sodium-based activators. • High alkalinity level (hazardous).	Danish et al. (2022).
Potassium silicate (K_2SiO_3)	0.51 (globally, 2021)	• Mixtures activated with potassium silicate exhibit great fire resistance and low thermal conductivity.	• Potassium-based activators are more costly than sodium-based activators.	Scanferla et al. (2022).

Continued on next page

Table 2.2 – continued from previous page

Alkaline activator	Production (Mt/year)	Benefits	Limitations	References
Sodium sulfate (Na_2SO_4)	11 (globally, 2013)	• Higher activator concentration, increased precursor fineness and high-calcium additives can improve the strength of sulfate-activated GPC significantly. • Produces higher workability and setting times than other activators. • Low drying shrinkage and good high-temperature resistance. • Suitable for specialized purposes (e.g., confinement of nuclear waste). • High availability and simple obtention process. • More practical and safer to use due to its relatively low alkalinity.	• The use of sodium sulfate-based activators yields lower early strength, especially when ambient-cured. This is due to their low alkalinity relative to other activators (e.g., NaOH, Na_2SiO_3). • Geopolymers activated with sodium sulfate require higher activator concentration to meet the same strength grade as geopolymers activated with NaOH and Na_2SiO_3. • Limited knowledge regarding permeability properties.	Adesina (2021).

2.4. Geopolymer concrete mixture design procedure

As with traditional concrete, designing GPC begins with establishing the desired mechanical performance, with compressive strength being a common standard target. However, formulating these materials can be more challenging than the established proportioning of PC concrete due to the many parameters involved in the geopolymers' matrix (Hassan et al., 2019b). There is a significant impact of raw material selection on GPC design, particularly chemical and mineralogical properties (García-Lodeiro et al., 2015). Parameters such as the solid precursor's reactive CaO/SiO_2 ratio and reactive SiO_2/Al_2O_3 ratio, as well as the influence of hydroxide, silicate and carbonate-based activators will each drive the behavior of the resultant GPC. Examples of theoretical and experimental methods for designing slag-based GPC mixtures are outlined in Shi et al. (2006), with these methods relying on statistics and experiments on the correlation between strength and constituent proportions, respectively, and the amounts of activator, fine aggregates and coarse aggregates are determined with volumetric relationships. Other works have suggested that calculating GPC's aggregate proportions is similar to PC methods. More recently, Lokuge et al. (2018) developed an approach for proportioning Class-F fly ash GPC based on a multivariate adaptive regression spline model. The model relies on contour plots of key relationships to achieve a targeted 28-day compressive strength, namely water-to-solid ratio, activator-to-fly ash ratio, Na_2SiO_3 to NaOH ratio, and NaOH concentration. The range of parameters that can be used for GPC mixture design drives highly tunable material performance for this class of materials.

Chapter 3

Impact of Mixture Parameters on the Mechanical Properties of GPC

The constituents selected both for the binder and for the other components of GPC will influence the material properties achieved. Here we focus on the effect of the alkaline activators, precursors, aggregates, water content, admixtures, pigments, and other parameters on key performance and constructability metrics used for GPC, namely workability, finishing, compressive strength, tensile strength, and flexural strength. A summary of findings is presented in Table 3.1, with each parameter discussed in more detail in the subsequent sections.

Table 3.1: Impact of different GPC mixture components on workability and finishing. This table presents a summary of the findings presented in Chapter 3. It highlights areas where clear trends are present in the literature for the effects of certain key parameters on GPC performance as well as where variable effects have been reported.

GPC parameter	**Workability**	**Finishing**	**Compressive strength**	**Tensile strength**	**Flexural strength**
Alkaline activator	$\updownarrow^{*}$	$\updownarrow^{*}$	$\updownarrow^{*}$	$\updownarrow^{*}$	$\updownarrow^{*}$
Precursor	$\updownarrow^{**}$	$\updownarrow^{**}$	$\updownarrow^{**}$	$\updownarrow^{**}$	$\updownarrow^{**}$
Aggregates	$\updownarrow$	$\updownarrow$	$\uparrow$	$\updownarrow$	$\updownarrow$
Increasing the water content	$\uparrow$	$\uparrow$	$\downarrow$	$\downarrow$	$\downarrow$

Continued on next page

Table 3.1 – continued from previous page

GPC parameter	Workability	Finishing	Compressive strength	Tensile strength	Flexural strength
Increasing the chemical admixtures content	↑	↑	↕***	↕***	↕***
Increasing the pigment content	↓	↓	↕	–	–
Heat curing	–	–	↑	↑	↑

↑ Indicates an improvement in the property.
↓ Indicates a deleterious effect on the property.
↕ Indicates improvement or deleterious impact on the property, depending on the mixture proportion.
* Depends on the concentration of the solution (see sections below).
** Depends on the type of precursor (see sections below).
*** Depends on the type and amount of superplasticizer.
– Data not reported in articles reviewed.

3.1. Workability

Workability, an indicator of the ease with which fresh concrete can be mixed, placed, consolidated, and finished to a homogeneous phase (Mather & Ozyildirim, 2002), reflects the mechanical work necessary to compact concrete without segregation (Shi et al., 2006). Due to the viscosity of the alkaline activators, GPC is generally less workable than PC of the same slump (Nguyen et al., 2020; Waqas et al., 2021). However, there is acceptable evidence of geopolymer flowability and workability (Shi et al., 2006), with workability being driven by several parameters, as discussed below.

3.1.1. Effect of the alkaline activator on workability.

The type of activators, their concentration, and the amount of solution will all drive changes in workability. A study by P. Nath and Sarker (2014) showed that the workability of GPC based on Class-F fly ash and a 14 M-combination of sodium hydroxide (NaOH) and sodium silicate (Na_2SiO_3) increases with a higher liquid content of alkaline activator solution, namely an increase in the alkaline activator content from 35% to 45% weight fraction of total binder more than doubled the workability of the GPC. As for the type of precursor, Bondar et al. (2018) showed an increase in the slump of alkali-activated

slag concrete with additions of sodium oxide (Na_2O) in the alkaline activator (a blend of NaOH and Na_2SiO_3). Further, Nematollahi and Sanjayan (2014) showed that employing the multi-compound activator (Na_2SiO_3/NaOH = 2.5) increased the relative slump and compressive strength by 41% and 57%, respectively, compared to using only NaOH (8 M) to activate Class-F fly ash GPC. In general, using Na_2SiO_3 produces mixes with good workability and strength (Pacheco-Torgal et al., 2015). Further, two recent studies selected a combination of NaOH and Na_2SiO_3 as the alkaline activator and explored the consequences of modifying the concentration of the NaOH solution: Nuruddin et al. (2011) and Nutakki et al. (2021). Both studies indicated that increasing the concentration of the NaOH solution diminishes the workability of Class-F fly ash GPC. Trends of Nutakki et al. (2021) are shown in Figure 3.1a.

3.1.2. Effect of the solid precursor on workability.

While myriad aluminosilicates could be leveraged for use in AAMs, low-calcium fly ash and ground granulated blast furnace slag (GGBFS) are the most commonly discussed precursors for GPC in the literature. It has been reported that the increase in the slag content decreases the workability of GPC (Nguyen et al., 2020; P. Nath & Sarker, 2014; Al-Majidi et al., 2016). This reduction has been ascribed to the precipitation of calcium silicate hydrate product of the quick reaction between the alkaline activator and the massive amount of calcium ions liquified from GGBFS (Nuaklong et al., 2016). For example, P. Nath and Sarker (2014), Al-Majidi et al. (2016), and Nguyen et al. (2020) all showed increasing the GGBFS percentage in fly ash-based GPC resulted in a stiffer, less workable mixture. Trends of Nguyen et al. (2020) are presented in Figure 3.1b. Though workability diminished by increasing the proportion of slag in the mixture, these studies reported an improvement in the compressive strength of their GPC. Inversely, Shi et al. (2006) reported that replacing 10–20% GGBFS with silica fume or fly ash in alkali-activated GGBFS-based GPC substantially increased workability.

3.1.3. Effect of the aggregates on workability.

The impact of fine and coarse aggregates on GPC workability is summarized in Shi et al. (2006) as follows: 1) an increase in the aggregate-to-binder ratio will yield a less workable mixture, 2) the closer the particles are to a spherical shape, the higher the workability, and 3) an excess of fine aggregate will produce an easier-to-place- (but more costly and absorbent) mixture. Furthermore, Pacheco-Torgal et al. (2015) reported that an aggregate-to-binder ratio of approximately 0.33 – which corresponds to a 75% proportion of aggregate in the mixture – yielded a high-workable, non-segregated fly ash-based GPC (slump of ∼240 mm), similar to PC. Beyond conventional aggregates, Thomas et al. (2022) conducted a study to assess the effect of recycled aggregates (RA) on the workability of GPC made with a blend of fly ash and GGBFS. These authors showed that higher porosity RA led to greater water absorption during batching and decreased workability. Still, using RA in surface-saturated dry conditions was beneficial to the workability of GPC (Thomas et al., 2022).

3.1.4. Effect of the water content on workability.

Multiple studies have reported that increasing water content improves the slump of GPC (Nguyen et al., 2020; Waqas et al., 2021; P. Nath & Sarker, 2014; Al-Majidi et al., 2016), as would be expected based on viscosity shifts. While the direct effects of increased water content vary based on other constituents selected, the literature suggests moderate increases in water content can drive notable changes in GPC workability. For example, Al-Majidi et al. (2016) showed the relative slump of fly ash GPC increased by 50% and 100% after the water-to-binder ratio was increased from 0.23 to 0.25 and 0.28, respectively. Similar trends in workability were shown by P. Nath and Sarker (2014) and Nguyen et al. (2020) for different GPC mixtures produced with fly ash and GGBFS. It must be noted that increasing the water-to-binder ratio prompted a lower compressive strength in each of these studies.

3.1.5. Effect of chemical admixtures and additives on workability.

Superplasticizers (SPs) – or high-range water-reducing admixtures – are commonly used to improve the workability of PC. Though SPs have also been implemented in GPC, their effectiveness might not be directly analogous to their effects on PC mixtures due to the different chemical compositions of these compounds (Nguyen et al., 2020). Nematollahi and Sanjayan (2014) showed the influence of SP on Class-F fly ash GPC varied depending on the alkaline activator. For example, in a mixture with NaOH (8 M), using naphthalene-based SP increased the relative slump of Class-F fly ash GPC by 136% and resulted in no reduction in the compressive strength. However, when using a multi-compound activator with Na_2SiO_3/NaOH = 2.5, naphthalene-based SPs and modified polycarboxylate SPs only improved the workability of GPC by 45% and 8%, respectively, and melamine-based SP led to a 3% decrease in the relative slump (see Figure 3.1c). All the SPs applied to the multi-compound activator decreased the compressive strength of their fly ash-based GPC. Similarly, Nguyen et al. (2020) examined the effects of five types of SPs (naphthalene, lignosulfonate, vinyl copolymer, polycarboxylate, and melamine) and suggested that naphthalene-based SPs are generally the most beneficial to GPC.

3.1.6. Effect of pigments on workability.

Producing colored GPC, commonly for aesthetic purposes, involves the addition of natural or synthetic pigments during the mixing stage, which affects the mechanical behavior of GPC (Mahmud & Abdulrehman, 2021; Hameed & Ali, 2021; Ghadban & Abdulrehman, 2022). Mahmud and Abdulrehman (2021) and Hameed and Ali (2021) studied the impact of adding four pigments – iron oxide hydroxide (yellow pigment), cobalt (blue pigment), iron oxide (red pigment), and chromium oxide (green pigment) – on metakaolin-based GPC. Their findings indicate that the GPC with no pigmentation exhibited a higher slump (40 mm) than the colored GPCs (see Figure 3.1d), which the authors assumed resulted from fine pigment particles contributing to a filler function. Interestingly, their results also show that 2% pigment content slightly increased compressive strength, again

attributed to a filler effect. Ghadban and Abdulrehman (2022) explored the influence of using chromium oxide (green pigment) and oxide hydroxide (yellow pigment) on fly ash-based GPC with consistent findings with Mahmud and Abdulrehman (2021) and Hameed and Ali (2021), i.e., a moderate reduction of workability and increase in strength with low levels of pigment.

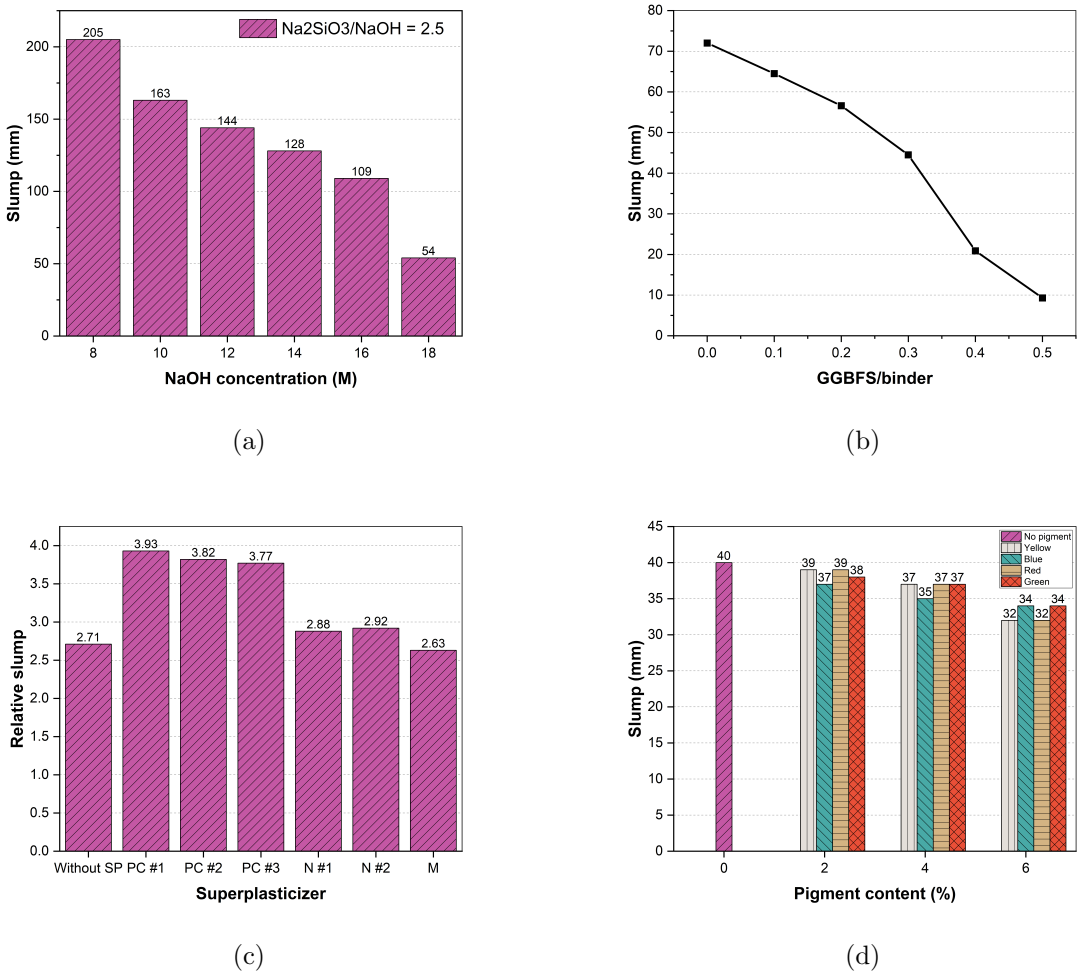

Figure 3.1: (a) Slump evolution of fly ash-based GPC in response to the alkaline activator concentration (Nutakki et al., 2021), (b) Effect of increasing the GGBFS/binder ratio on the slump of fly ash and GGBFS-based GPC (Nguyen et al., 2020), (c) Effect of different SPs on the relative slump of fly ash-based GPC. SP = Superplasticizer, PC = Polycarboxylate-based superplasticizer, N = Naphthalene-based superplasticizer, M = Melamine-based superplasticizer (Nematollahi & Sanjayan, 2014), (d) Effect of different pigments on the slump of metakaolin-based GPC (Mahmud & Abdulrehman, 2021; Hameed & Ali, 2021).

Notably, the parameters influencing the workability of GPC, a paramount property for constructability, fall into specific ranges, yet results can vary depending on other GPC characteristics. For example, there is consensus in the literature that the optimal NaOH concentration lies between 6 M and 18 M, and as seen from Figure 3.1a, the NaOH solution concentration was raised from 8 M to 18 M to assess the slump of fly ash- based GPC, with results ranging between ∼50 and ∼200 mm (Nutakki et al., 2021). However, other studies (e.g., Nuruddin et al. (2011)) considered a similar range (8–12 M), found the same trend, and yet obtained different slump results (e.g., 600–800 mm) due to other variations in the constituents and mixtures. This highlights the importance of considering all the parameters influencing GPC. In addition, it has been noted that sodium-based compounds (NaOH and Na_2SiO_3) are the most extensively used alkaline activators for GPC manufacturing, with NaOH-to-Na_2SiO_3 ratios ranging from 1.5 to 3.0. From Figure 3.1b, the GGBFS replacement in fly ash-based GPC reached up to 50%, a representative upper limit for the literature, which has shown replacements between 10 and 50% (e.g., Al-Majidi et al. (2016)). Though the trend shown in Figure 3.1b is consistent with other studies, a change in the aluminosilicate sources (e.g., adding silica fume) can alter the workability behavior significantly, as shown by Shi et al. (2006). Lastly, to the authors' knowledge, very few studies have explored the effects of pigments on the workability of any kind of GPC.

3.2. Compressive strength

Compressive strength is one of the most commonly analyzed parameters for GPC concrete, and it can be carefully tuned based on the use of different mixture parameters, as discussed below.

3.2.1. Effect of the alkaline activator on compressive strength.

The compressive strength of GPC is highly influenced by the type of alkaline activator, its concentration, and its dosage (Pacheco-Torgal et al., 2015). Consequently, many

authors have investigated the effects of these parameters (Nematollahi and Sanjayan (2014); Nuruddin et al. (2011); Nutakki et al. (2021); Waqas et al. (2021)). A few examples include Nematollahi and Sanjayan (2014), who showed that using a multi-compound sodium-based activator (Na_2SiO_3/NaOH = 2.5) improved the compressive strength of Class-F fly ash GPC (an increase of over 50% relative to using only NaOH (8 M)). Nuruddin et al. (2011) found that increasing the NaOH concentration from 8 to 12 M improved the compressive strength, whereas increasing the concentration from 12 to 14 M decreased the compressive strength of self-compacting fly ash-based GPC. Similarly, Waqas et al. (2021) observed that the compressive strength of fly ash and slag-based GPC increased as the NaOH concentration increased from 10 M to 12 M; however, unlike Nuruddin et al. (2011), the strength improved from 12 to 14 M (see Figure 3.2a), suggesting the other constituents selected in the GPC will influence the tipping point of desired molarity. Further, Nutakki et al. (2021) noted that sodium-based alkaline activators (NaOH and Na_2SiO_3) produced higher compressive strength than potassium-based alkaline activators (KOH and K_2SiO_3) in GPC made with fly ash.

3.2.2. Effect of the solid precursor on compressive strength.

Several aspects of the solid precursor can drive changes in the compressive strength of GPC. As could be expected, the composition of the solid precursor will contribute to strength development. For example, P. Nath and Sarker (2014) showed an approximate 10 MPa for every 10% increment in the GGBFS content of fly-ash GPC (see Figure 3.2b). Similar results were shown by Nguyen et al. (2020) when exploring the use of GGBFS instead of fly ash. In addition to the varying composition, simply increasing the fineness (or reducing the particle size) can increase the reactivity and strength (particularly early-age strength) of cementitious systems; however, exceeding a certain value can escalate the water demand, which can reduce the strength (Pacheco-Torgal et al., 2015; Shi et al., 2006). For example, (Pacheco-Torgal et al., 2015) reported that the optimal fineness of blast furnace slag ranges between 400 to 550 m^2/kg and that replacing slag with ultra-fine

slag (1500 m^2/kg) significantly improves the early age strength of GGBFS-based GPC. Similar results have been reported by Nguyen et al. (2020), who noted finer particles of fly ash can increase compressive strength for the same age mixtures.

3.2.3. Effect of the aggregates on compressive strength.

Aggregate features can highly affect the hardened properties of GPC, including compressive strength. Sreenivasulu et al. (2015) assessed the mechanical properties of Class-F fly ash and GGBFS-based (50:50) GPC with different blends of fine aggregates. These authors showed even with consistent levels of coarse aggregate, changing the characteristics of the fine aggregate could increase strength; however, excessive levels of fine particles should be avoided. Further, the composition, shape, and hardness of the aggregates can influence mechanical properties, as was shown in a study by Mermerdaş et al. (2017). These authors examined three types of aggregates (river sand, crushed limestone, and combined sand and limestone) to prepare fly ash-based geopolymer mortars and showed mixtures with crushed limestone exhibited the highest compressive strength. In contrast, those with river sand displayed the lowest compressive strength – a factor attributed to the angular shape of crushed limestone contributing to better bond strength.

3.2.4. Effect of the water content on compressive strength.

Increasing the water-to-binder ratio in GPC yields a lower compressive strength, similar to PC concrete (Nguyen et al. (2020); Al-Majidi et al. (2016)). Nguyen et al. (2020) exhibited this characteristic by examining Class-F fly ash GPC for multiple water-to-binder ratios (0.20, 0.25, 0.30) and showing a near linear reduction in compressive strength with increasing water-to-binder ratio. Comparable results have been shown by others, such as Al-Majidi et al. (2016), who examined water-to-binder ratio variations from 0.23 to 0.25 and 0.28 in fly ash-based GPC (see Figure 3.2c).

3.2.5. Effect of chemical admixtures and additives on compressive strength.

There are many chemical admixtures that are used in PC concrete and could be used in GPC as well. Here, we focus on the use of superplasticizers (SPs), which are commonly used to enhance workability, but they also affect compressive strength. Nematollahi and Sanjayan (2014) showed that polycarboxylate and melamine-based SPs produced detrimental effects on the compressive strength of fly ash-based GPC. Interestingly, these authors noted that adding naphthalene-based SPs to a GPC mixture activated with NaOH (8 M) did not affect compressive strength; yet it resulted in a substantial loss in strength recorded for mixtures activated with a blend of Na_2SiO_3 and NaOH. Nguyen et al. (2020) further showed the variability in the effects of SPs on strength by examining the use of two naphthalene and two polycarboxylate-based SPs in GPC made with a blend of fly ash and GGBFS, with results showing compressive strength variations within 5 MPa of the control mixture with no SP. This behavior is attributed to the chemically unstable condition in which most SPs have to operate – a consequence of the high alkalinity (pH > 13) induced by the activators (Nguyen et al. (2020); Nematollahi and Sanjayan (2014)). When applied with a multi-compound activator, naphthalene and melamine-based SPs produced greater declines in compressive strength (40–50%) than polycarboxylate-based SPs (15–30%), in addition to having a lower impact on workability. The polycarboxylate's higher plasticizing effect and less adverse consequences on compressive strength are ascribed to its structure's lateral chains, which cause steric and electrostatic repulsions. In the case of using NaOH as the activator, the literature has shown that naphthalene-based admixtures are the only group that is chemically stable for geopolymers (e.g., Nguyen et al. (2020); Nematollahi and Sanjayan (2014)).

3.2.6. Effect of pigments on compressive strength.

As with workability, pigments can have some effect on mechanical properties. Mahmud and Abdulrehman (2021) and Hameed and Ali (2021) reported minimal changes in the compressive strength of metakaolin-based GPC with yellow, blue, red and green pigments

in various dosages (2, 4, and 6% wt. of metakaolin). The authors noted some mild benefits to the compressive strength of mixtures with 2% pigment (and a moderate loss of strength at greater levels), which was attributed to a filler effect from the pigment at low levels and an accumulation of particles, leading to segregation, at higher levels. Similarly, trends of modest benefits at low pigment levels and some loss of strength at high pigment levels in fly ash-based GPC were reported by Ghadban and Abdulrehman (2022).

3.2.7. Effect of curing conditions on compressive strength.

As Kuenzel et al. (2012) noted, the mechanical properties of geopolymer binders can be greatly influenced by the curing conditions if temperature is needed to support the formation of appropriate mineral phases in the paste. Common PC curing processes are also applicable to alternative binders (e.g., steam and autoclave curing), but water curing conditions could lead to premature leaching and loss of strength for GPC (Pacheco-Torgal et al., 2015). For example, Nguyen et al. (2020) applied three different ambient/low-temperature curing methods to GPC made with fly ash and GGBFS that integrated a variation of curing temperatures and sealing regimes before exposing the GPC to ambient conditions. The low-temperature curing these authors explored (10 °C) hindered strength development (see Figure 3.2d). These authors also showed differences in the effects of using moisture in curing; in the cases they explored, the use of air curing improved the compressive strength of GPC containing fly ash only, whereas the water curing was more beneficial to the blended fly ash with GGBFS GPC. P. Nath and Sarker (2014) explored higher temperature curing (60 °C for 24 h) in GPC made with fly ash and GGBFS and showed mixtures cured at high-temperature achieved an elevated early-age strength relative to the same mixtures cured at ambient temperature (see Figure 3.2d).

As shown in Figure 3.2, the compressive strength variation of different GPC specimens can range from ordinary concrete grade (∼10 MPa) to high-strength grade (∼70 MPa), with this wide spectrum being determined by several mixture parameters or curing conditions, as discussed before. In addition to the strength enhancement with time, all the trends

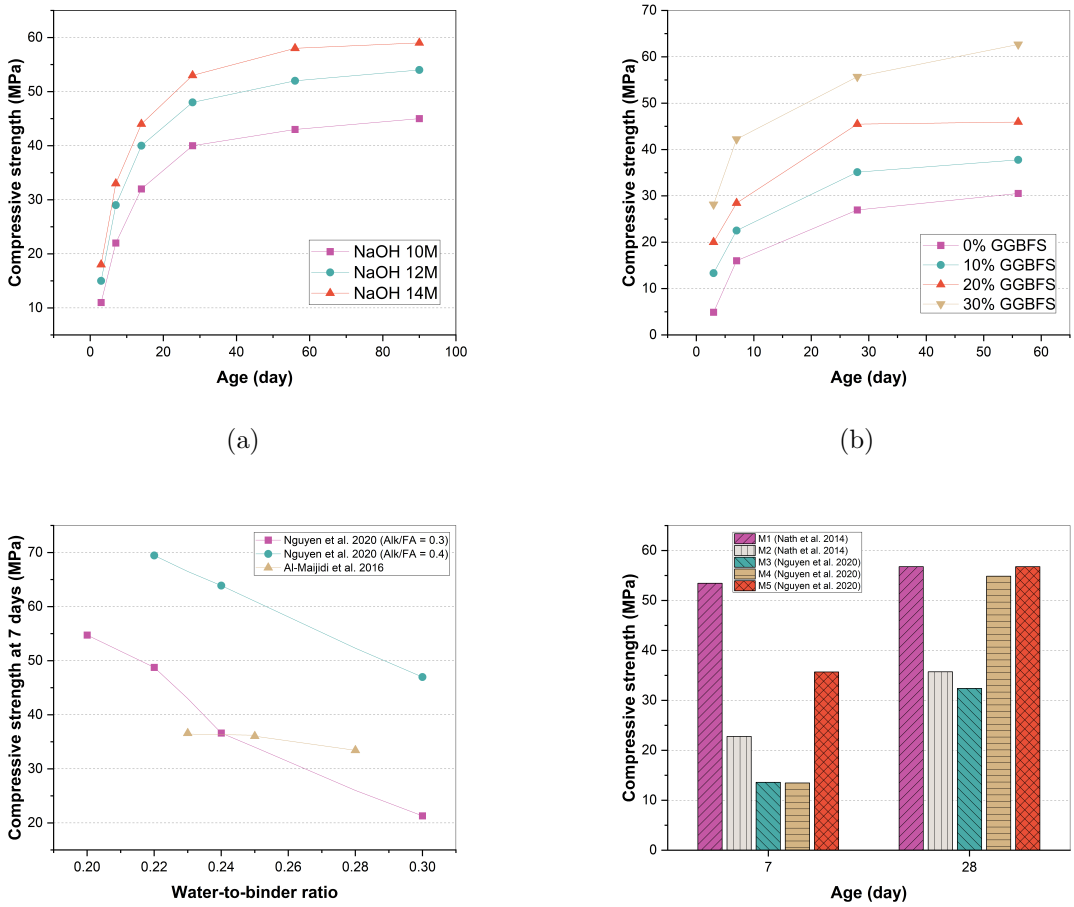

Figure 3.2: (a) Compressive strength at different ages for class-F fly ash-based GPC activated with various sodium hydroxide concentrations (10–14 M) (Waqas et al., 2021), (b) Effect of increasing the GGBFS replacement in fly ash-based GPC (P. Nath & Sarker, 2014), (c) Evolution of the compressive strength of Class-F fly ash GPC in response to water to binder ratio variation (Nguyen et al., 2020; Al-Majidi et al., 2016), (d) Effect of different curing conditions on the compressive strength of fly ash and GGBFS-based GPC. M1 = sealing the samples and curing them at 10-20 ℃ all the time before testing, M2 = sealing and curing the samples at 10 ℃ for 7 days before air-dried at 20 ℃, M3 = sealing and curing the samples at 20 ℃ for 24 h before air-dried at 20 ℃, M4 = high-temperature curing (60 ℃ for 24 h) (Nguyen et al., 2020; P. Nath & Sarker, 2014).

found in the literature also agree with the compressive strength improvement prompted by the NaOH concentration change from 8 M to 10 M and from 10 M to 12 M, but with Waqas et al. (2021) being the only study finding and enhancement from 12 M to 14 M (see Figure 3.2a). Further, Figure 3.2b, which displays typical GGBFS replacement

dosages in fly ash-based GPC, shows a consonant tendency with other studies (e.g., Nguyen et al. (2020)), with Nguyen et al. noting that GGBFS replacements over 50% have negligible effects on compressive strength. Figure 3.2c illustrates the harmonized influence of the water-to-binder ratio on the compressive strength of low-calcium fly ash GPC, with different studies testing similar ratios (water-to-binder ratios of 0.20–0.30), but slightly lower than those observed in Lokuge et al. (2018) (water-to-binder ratios of 0.15–0.45). The wide variety of curing methods available for GPC is displayed in Figure 3.2d, noting that certain curing conditions are needed to drive desired reactions. Though some mixtures cured at ambient temperature exhibited lower compressive strength, this strength was comparable with the strength of PC concrete in normal curing conditions. Thus, GGBFS and fly ash-based GPC cured at ambient temperature can be adequate for construction in-situ where heat curing is not easily available.

3.3. Tensile strength

Tensile strength, while not as regularly studied as compressive strength, has often been shown to have better characteristics in GPC than in conventional PC concrete. Concurrently, the improved tensile strain capacity of GPC has been ascribed to increased creep, lower elastic modulus, and improved tensile strength of GPC (Pacheco-Torgal et al., 2015). As with other properties, the tensile strength of GPC is driven by several parameters.

3.3.1. Effect of the alkaline activator on tensile strength.

Alkali-activator concentration and type have been shown to drive changes in GPC tensile strength. Verma and Dev (2021) varied the NaOH concentration from 8 to 16 M and showed general trends suggesting increasing the concentration of NaOH in the alkaline activator enhances the tensile strength of GPC made with fly ash and GGBFS (see Figure 3.3a). Such results align with other studies, such as Bellum et al. (2022), who showed improved tensile strength with increasing the NaOH concentration from 8 to 10 M in fly

ash and GGBFS-based GPC. Verma and Dev (2021) also showed varying the NaOH-to-Na_2SiO_3 ratio from 0.5 to 3.0 led to shifts in tensile strength, with their results showing a peak tensile strength at $NaOH/Na_2SiO_3 = 2.5$.

3.3.2. Effect of the solid precursor on tensile strength.

The effects of varying solid precursors on tensile strength have been well-reported in the literature, particularly for fly ash and GGBFS (Nutakki et al., 2021; Bellum et al., 2022; Verma & Dev, 2022a). As with compressive strength, the beneficial effects of using GGBFS have been reported by several authors. For example, Bellum et al. (2022) found that increasing the GGBFS content in fly ash-based GPC augmented the tensile strength of the specimens significantly – a 2 – 6 MPa increase in tensile strength for every 10% of fly ash replaced with GGBFS – contributing an up to 80% increase in tensile strength for mixtures with 40% GGBFS activated with NaOH 8 and 10 M (see Figure 3.3b). Similarly, Verma and Dev (2022a) showed the tensile strength of fly ash-GGBFS blended GPC activated using NaOH and Na_2SiO_3 also benefited from some addition of GGBFS, albeit at a slightly lower replacement level than Bellum et al. (2022). In line with these authors, Nutakki et al. (2021) observed that gradually increasing the fly ash content from 300 to 550 kg/m^3 diminished the split-tensile strength of fly ash and GGBFS-based GPC activated with NaOH and Na_2SiO_3 by 39%.

3.3.3. Effect of the aggregates on tensile strength.

As was noted for compressive strength, aggregate characteristics can drive changes in the tensile strength of GPC. Sreenivasulu et al. (2015) showed that granite slurry replacement of fine aggregates could have beneficial effects if limited to moderate levels, with benefits found when aggregates can contribute to enhancements in the interfacial transition zone and, thus, the tensile strength of low-calcium fly ash and GGBFS-based GPC. Test results showed that after 7, 28 and 90 days, the split tensile strength of the GPC increased with the ground slurry content up to 40%, decreasing notably after exceeding this percentage. Mermerdaş et al. (2017) showed the tensile strength of geopolymer mortars varied when

using river sand, crushed limestone, and a combination of sand and limestone as fine aggregates, with the greatest tensile strength being reported with the use of crushed limestone (similar to their compressive strength results). This behavior can be attributed to the angular shape of crushed limestone, which improves the bond of the mixture.

3.3.4. Effect of the water content on tensile strength.

Water content in mixtures can again be a driver for mechanical characteristics. Aliabdo et al. (2016) studied the effect of additional water content on the tensile strength of fly ash-based GPC activated with NaOH and Na_2SiO_3. Notably, these authors held all other mixture parameters constant (NaOH molarity, admixture content, NaOH-to-Na_2SiO_3 ratio, and solution-to-fly ash ratio) and varied water content between 10 and 35 kg/m^3. Their results showed that not only does an increased water content reduce strength, as would be expected if it led to increased porosity, but the reduction in tensile strength was more significant than that observed for compressive strength.

3.3.5. Effect of chemical admixtures and additives on tensile strength.

The impact of chemical admixtures on the tensile strength of GPC has been documented in the literature (Aliabdo et al., 2016; Verma & Dev, 2022b). Aliabdo et al. (2016) explored the effect of using a Type F naphthalene-based superplasticizer on the tensile properties of fly ash-based GPC. While the authors noted moderate improvements in tensile strength with a dosage of SP (2.5 kg/m^3), higher levels led to a proportional decrease in tensile strength, with the loss of tensile strength being more pronounced than reductions for compressive strength. Verma and Dev (2022b) evaluated a sulfonated naphthalene-based SP and showed that oven-cured specimens exhibit higher tensile strength than those cured at ambient temperature, with 1% SP as an optimal dosage (see Figure 3.3c).

3.3.6. Effect of curing conditions on tensile strength.

As alluded to in the presentation of chemical additives, curing conditions can also drive shifts in tensile strength. Over a series of experiments conducted by Verma and Dev in Verma and Dev (2021, 2022a) and Verma and Dev (2022b), the authors demonstrated that oven curing at high temperatures (∼60 °C) improves the tensile strength of fly ash and GGBFS-based GPC at all ages compared with curing at ambient temperature. Triwulan et al. (2017) reported consistent findings when assessing the tensile strength of fly ash-based GPC specimens subjected to different curing conditions – normal curing (i.e., ambient temperature curing) and heat curing at 40 °C, 60 °C, and 80 °C – showing that curing at higher temperatures produces GPC with higher tensile strength regardless of the Na_2SiO_3-to-NaOH ratio (see Figure 3.3d).

Figure 3.3 summarizes key aspects relating to the splitting-tensile strength of myriad GPC mixtures. Notably, there is extensive variation in this mechanical property, with results ranging from 1 to 35 MPa. Similarly, the parameters determining the splitting tensile strength also vary in a broad manner, each influencing the mechanical behavior and having a combined effect. Figure 3.3b provides an interesting example of the cumulative effects of GGBFS replacement of fly ash in GPC and different NaOH concentrations, namely 8 M and 10 M. It can be noted that GPC can be tuned to exhibit comparable or even significantly superior performance in tension relative to PC concrete based solely on the variation of these parameters. The effects of different sulfonated naphthalene-based SP dosages on tensile strength were studied by Aliabdo et al. (2016) and Verma and Dev (2022b) (see Figure 3.3c); however, these authors did not consider finding the optimum dosages of other SPs found in the literature (e.g., melamine-based and polycarboxylate SPs). In Figure 3.3d, the influence of different curing temperatures on splitting-tensile strength is portrayed, once again showcasing the broad possibilities of curing conditions available for GPC. Notably, the upper limits for temperature (80 °C) and the Na_2SiO_3 to NaOH ratio (2.5) are typical in the literature (e.g., Hassan et al. (2019a)).

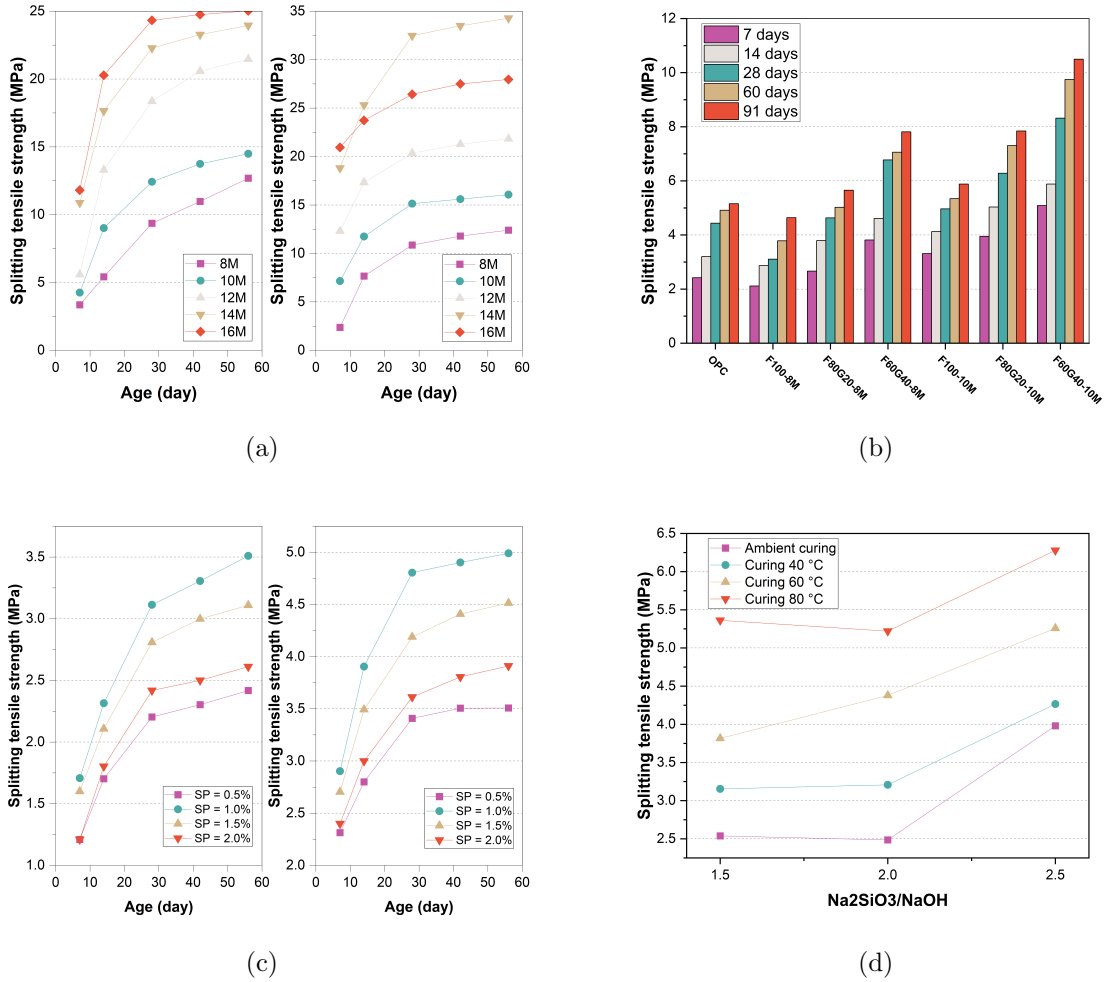

Figure 3.3: (a) Evolution of the splitting tensile strength of ambient-cured GPC (left) and oven-cured GPC (right) in response to the NaOH concentration (Verma & Dev, 2021) (specimens made with a blend of fly ash and GGBFS), (b) Splitting tensile strength of fly ash-based GPC with different GGBFS replacements and NaOH concentrations compared to PC concrete at different ages (Bellum et al., 2022), (c) Effect of various superplasticizer (SP) dosages on the tensile strength of ambient-cured GPC (left) and oven-cured GPC (right) (Verma & Dev, 2022a) (specimens made with a blend of fly ash and GGBFS), (d) Splitting tensile strength of fly ash-based GPC cured at different temperatures for multiple Na_2SiO_3/NaOH ratios (1.5, 2.0, 2.5) (Triwulan et al., 2017).

3.4. Flexural strength

The flexural strength, reflecting the stress a material can withstand in bending, is a crucial consideration in the design of structural elements, such as beams, columns, and slabs, as well as for pavements. As behavior in bending is a reflection of tensile and compressive action, trends for flexural strength are consistent in the preceding sections.

Ghafoor et al. (2021) highlighted the effects of several alkaline activator parameters on the flexural strength of GPC, namely NaOH concentration, sodium silicate-to-sodium hydroxide ratio (Na_2SiO_3/NaOH) and alkaline activator-to-fly ash ratio. The authors experimentally investigated the use of five NaOH concentrations (8, 10, 12, 14 and 16 M), three Na_2SiO_3/NaOH ratios (1.5, 2.0 and 2.5), and three alkaline activator-to-fly ash ratios (0.4, 0.5 and 0.6) in ambient-cured Class-F fly ash GPC specimens. Their results showed the flexural strength of GPC increases as the NaOH concentration increases (see Figure 3.4a), which the authors posited was a result of a catalyzed N-A-S-H gel formation leading to a more robust matrix. Increasing the Na_2SiO_3/NaOH from 1.5 to 2.0 reduced the flexural strength of GPC activated with low NaOH concentrations (8, 10 and 12 M) and enhanced the flexural strength of the specimens activated with high concentrations (14 and 16 M), whereas ratios of Na_2SiO_3/NaOH from 2.0 to 2.5 diminished the flexural strength. The flexural strength of GPC increased ∼20% as the activator-to-precursor ratio increased from 0.4 to 0.5, but a ∼1% reduction in strength was noted when the ratio was further increased from 0.5 to 0.6. Each of these factors suggests the high level of control a designer could have over the flexural strength attained for GPC.

GGBFS as a solid precursor was commonly reported as resulting in improved strength. Bellum et al. (2022) showed fly ash-based GPC mixtures with 10, 20, 30 and 40% of GGBFS activated with NaOH 8 M exhibited flexural strength improvements of 9, 25, 35 and 71%, respectively. Those activated with NaOH 10 M showed improved flexural strengths by 19, 34, 55 and 81% compared to the mixture with only fly ash, respectively. Verma and Dev (2022a) showed similar trends in fly ash and GGBFS-based GPC, but they noted a slightly lower optimal level of GGBFS.

As has been presented for tensile and compressive strength, appropriate aggregate gradation (i.e., without too much fine aggregate) contributed to increased flexural strength (Sreenivasulu et al., 2015), as can low levels of pigments (typically less than 2%) (Mahmud & Abdulrehman, 2021; Hameed & Ali, 2021; Ghadban & Abdulrehman, 2022). Yet

strength has an adverse response to extra water content. A study by P. Nath and Sarker (2017) explored the evolution of flexural strength as a function of water content in ambient-cured GPC made with fly ash and GGBFS. Their results indicate that, compared to the control sample, the mixture with additional water (6 kg/m^3) showed around 30% less 28-day and 90-day flexural strength.

As shown in previous sections, SPs can also affect the flexural strength of GPC. For example, Verma and Dev (2022b) characterized the flexural strength of fly ash and GGBFS-based GPC with multiple sulfonated naphthalene-based SP contents (0.5 %, 1%, 1.5% and 2%). The authors showed the flexural strengths of the ambient-cured samples were lower than those of the oven-cured specimens at the same age. Moreover, the samples of both curing methods reached their highest flexural strength with 1% of SP, followed by 1.5 and 2%, regardless of age. (Henigal et al., 2017) also showed the potential benefits of SP. Namely, these authors found that increasing the percentage of Type G SP (Viscocrete-3425) from 5 to 7% improved the 28-day flexural strength of self-compacting GPC by around 5%.

Further, if heat-curing can contribute to desired mineral phase formation or increase the rate of reactions, there can be beneficial effects on flexural strength. For example, Hassan et al. (2019a) examined the impact of two curing conditions (ambient curing and curing at 75 °C for 26 h) on the flexural strength of GPC made with low-calcium fly ash. Results showed that ambient-cured samples have lower flexural strength than oven-cured samples at all ages, with higher stretch achieved at later ages (see Figure 3.4b).

Figures 3.4a and 3.4b show flexural strength variations within ∼1.5 MPa and ∼7.5 MPa, driven by mixture design parameters, namely the alkaline activator/fly ash ratio, the NaOH concentration, and the curing conditions. In Figure 3.4a, the alkaline activator/fly ash ratio between 0.4 and 0.6 is consistent with other ranges found in the literature for fly ash-based GPC (e.g., 0.2–0.8 (Nutakki et al., 2021)). Further, the NaOH concentration range from 8 to 16 M is in agreement with other studies (e.g., Lokuge et al. (2018)). The

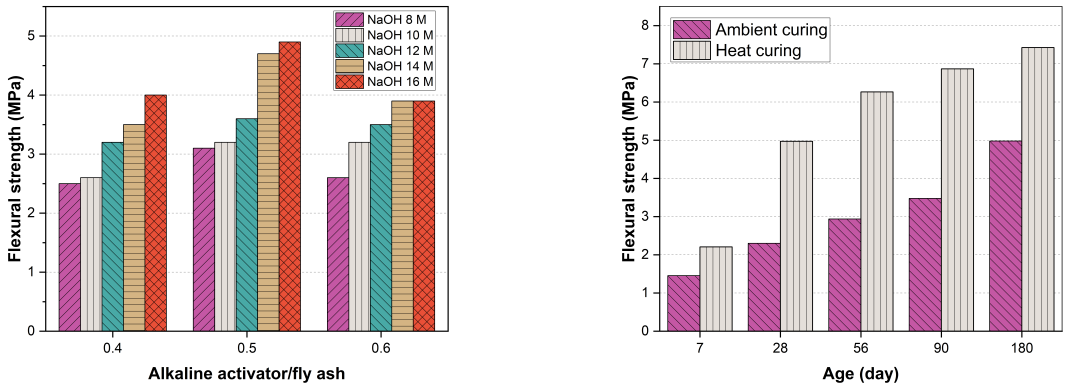

(a) (b)

Figure 3.4: (a) Evolution of the flexural strength of fly ash-based GPC in response to the NaOH concentration for various alkaline activator/fly ash ratios (0.4, 0.5, 0.6) (Ghafoor et al., 2021), b) Flexural strength for ambient-cured and oven-cured (75 ℃) fly ash-based GPC (Hassan et al., 2019a).

flexural strength response to different curing temperatures is shown in Figure 3.4b, with these temperatures observed in other studies (e.g., Triwulan et al. (2017)). Interestingly, the flexural strength shows a notable improvement between ages 7 and 28 days for oven-cured fly ash-based GPC, and between 90 and 180 days for ambient-cured GPC.

3.5. Finishing

Finishing of concrete conventionally uses tools such as screeds, trowels, darbies, bull floats, etc., to achieve a smooth and sturdy surface by leveling the fresh concrete. Appropriate workability, homogeneity, and setting time facilitate finishing processes Kwasny et al. (2018). As with other constructability factors, the finishing of GPC is susceptible to constituents selected and can vary from PC concrete.

3.5.1. Effect of the alkaline activator on finishing.

As discussed in previous sections, high concentrations in the alkaline activator can yield viscous mixtures. Thus, placing and finishing GPC with high alkaline activator concentration (i.e., viscous and with poor workability) can be challenging. Tempest et al.

(2015) reported that the Class-F fly ash-based GPC used in their project was significantly more viscous than the PC, making it difficult to use conventional tools. Likewise, Andrews-Phaedonos (2011) claimed that the fly ash and GGBFS-based geopolymer mixture they obtained required a water sprayer to reduce the surface's stiffness and facilitate the mixture's finishing. However, constituents selected and project requirements can drive different effects. Montes and Allouche (2012) and Bligh and Glasby (2013) have demonstrated GPC, as well as geopolymer mortar and grout, can be mixed, pumped, placed, sprayed and finished with the same equipment and procedures used for PC.

In addition, the type of alkaline activator can alter the initial and final setting times, thus, modifying the time available to complete the placing and finishing of the fresh concrete (P. Nath & Sarker, 2014; Tennakoon et al., 2016). According to P. Nath and Sarker (2014), the initial setting time of GPC made with a blend of Class-F fly ash and GGBS increased roughly 33% for every 5% increase in the alkaline activator (NaOH and Na_2SiO_3) to binder ratio, and the final setting time showed similar behavior (see Figure 3.5a). Furthermore, Tennakoon et al. (2016) observed that the initial and final setting time of GPC made with fly ash and GGBFS varied with the type of solid activator. They found that using pentahydrate sodium metasilicate resulted in twice as much setting time than anhydrous sodium metasilicate. The longest setting time obtained in this study was 200 minutes for GPC with 90% fly ash and 10% GGBFS activated with pentahydrate sodium metasilicate.

3.5.2. Effect of the precursor on finishing.

Because solid precursors used in GPC can drive changes in workability, these, in turn, can affect finishing. Xie et al. (2019) claimed that the increase in the content of GGBFS in fly ash-based GPC substantially reduced both the initial and final setting time of the fresh mixture, which can significantly impact the finishing process. These times represent a considerable reduction of the time available for finishing compared to the PC studied in their research, namely an 86–97% reduction in initial and final setting times were noted

(see Figure 3.5b). Similarly, Tennakoon et al. (2016) reported that for the activators they implemented (anhydrous sodium metasilicate and pentahydrate sodium metasilicate), an increase in the slag content generated a decrease in the setting time of GPC made with Class-F fly ash and GGBFS.

3.5.3. Effect of the aggregates on finishing.

As is the case with PC concrete, aggregates can influence GPC finishing. In the implementation described in Andrews-Phaedonos (2011), the finishing of the geopolymer mixture was complicated due to the handling of the coarse aggregate, and the use of an expanded mesh roller was necessary to complete the finishing. In another case study, Tempest et al. (2015) highlighted the importance of regulating the moisture of the aggregates in fly ash-based GPC since the alkaline activator in liquid form also contributes to the mixture's workability.

3.5.4. Effect of the water content on finishing.

Water content plays a crucial role in obtaining GPC with a desirable level of workability and adequate setting time; thus, it also drives changes in placing and finishing. For example, Xie et al. (2019) point out that low water-to-binder ratios may produce inappropriate setting times: they obtained a setting time of less than 20 min with a water-to-binder ratio of 0.3 for a GPC with a 75% GGBFS-to-fly ash ratio. Placing and finishing this concrete would be challenging for practitioners due to the limited time to perform these tasks. In addition, they reported reactions of 25% and 39% in the initial setting time when the water-to-binder ratio of their mixture was changed from 0.5 to 0.4 and 0.3, respectively (see Figure 3.5c). Similarly, higher water content resulted in longer setting times in the project carried out by Andrews-Phaedonos (2011). Here, it was found that the stipple finish for their panel application was more effective than the broom finish, and the author stated that optimal finishing could be achieved by screeding and waiting as much as possible for the final finish.

3.5.5. Effect of chemical admixtures and additives on finishing.

As noted previously, using SPs can enhance workability, which can facilitate the placement and finishing of GPC in certain scenarios, and SPs can modify setting time, also benefiting finishing. Results from Xie et al. (2019) exhibited initial setting times within 5 min for fly ash and GGBFS-based GPC mixtures without a retarding water reducer. Such setting times would be problematic as it would be impossible to finish mixing and handling the fresh concrete at a construction site.

3.5.6. Effect of pigments on finishing.

As concluded by many studies (Mahmud & Abdulrehman, 2021; Hameed & Ali, 2021; Ghadban & Abdulrehman, 2022), adding pigments to the mixture reduces the workability of metakaolin-based GPC and fly ash-based GPC, regardless of color. Still, differences are minute and likely not to influence finishing. The impact of pigments on the setting time of GPC is not well reported in the literature.

Figure 3.5 showcases the noteworthy GGBFS replacement percentages found in the study by Xie et al. (2019), with up to 75% of fly ash replaced with slag to control the initial and final setting times of GPC (Figure 3.5b). It was previously noted that GGBFS replacements over 50% did not drive changes in the compressive strength of fly ash-based GPC (Nguyen et al., 2020); however, it could lead to a substantial decrease in the initial and final setting times, key parameters for constructability. Similarly, the maximum water-to-binder ratio in Xie et al. (2019) (0.5) is slightly higher than the ones observed in other studies (e.g., Lokuge et al. (2018); Nguyen et al. (2020); Al-Majidi et al. (2016)).

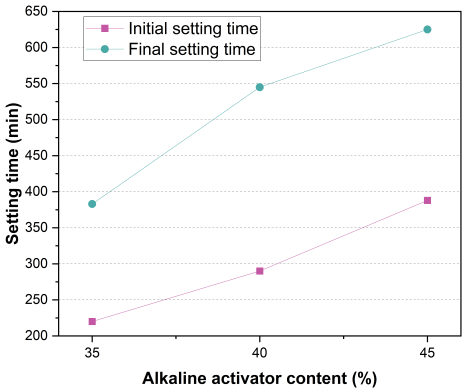

(a)

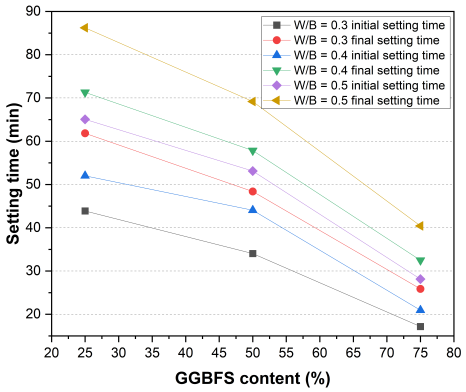

(b)

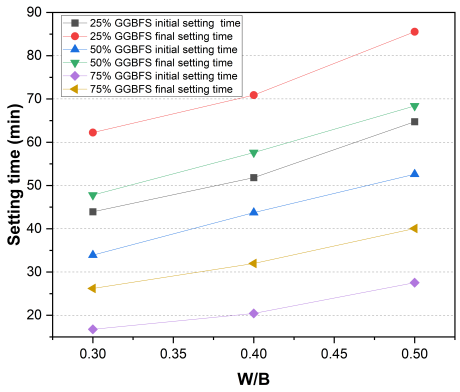

(c)

Figure 3.5: (a) Effect of the alkaline activator content on the setting time of fly ash and GGBFS-based GPC (P. Nath & Sarker, 2014), (b) Evolution of the initial and final setting times of fly ash-based GPC with the GGBFS replacement for different water to binder ratios (W/B) (Xie et al., 2019), (c) Initial and final setting times of fly ash-based GPC as a function of the water to binder ratio (W/B) for various GGBFS replacement levels (Xie et al., 2019).

Chapter 4

Durability

Most concrete applications are long-lived, stretching from several decades to over one hundred years (Kapur et al., 2008). As a result, the durability of alternatives to PC concrete is often highlighted as an area of interest.

4.1. Resistance to chloride ingress

Even in the high alkalinity environment of GPC, chloride ingress can contribute to steel reinforcement corrosion and expensive reparation procedures (Shi et al., 2006). While a prevalent way of testing concrete durability to such ingress is through the rapid chloride permeability test, this test has a weak correlation to the direct diffusion resistance to chloride permeability of AAMs (Provis et al., 2015). The alkali activator can alter the pore chemistry and compromise the rapid chloride permeability test, but other test methods have emerged as potential solutions for measuring chloride resistance, such as alternative accelerated chloride migration tests (Provis et al., 2015). In a study by Alzeebaree et al. (2020), fiber-reinforced GPC exhibited better corrosion resistance than PC concrete after confinement with carbon and basalt under chloride attack. It was observed that unconfined GPC and PC concrete reduced their 90-day compressive strength by 11.4% and 16.6% due to chloride attack, respectively. The confined GPC specimens showed

1.5 – 3 times greater strength than unconfined specimens subjected to the same testing conditions. However, more work is needed in this area.

4.2. Resistance to carbonation

Carbonation of PC concrete can affect several properties, including increased susceptibility to steel corrosion, loss of strength, increased pore volume, and shrinkage (Shi et al., 2006; Pacheco-Torgal et al., 2015; Provis et al., 2015), but AAMs differ from conventional PC's carbonation. Namely, in the case of PC concrete, carbonation is a mechanism predominantly interacting with portlandite ($Ca(OH)_2$), which in turn lowers the pH of the pore solution and compromises the reinforcing steel's passivation layer, facilitating steel corrosion (Pouhet & Cyr, 2016). The carbonation of alkali-activated binders, on the other hand, encompasses two steps (Pacheco-Torgal et al., 2015): (1) the carbonation of the pore solution, which reduces the pH level and precipitates sodium-rich carbonates; and (2) the decalcification of calcium-rich systems, especially C-S-H. For example, the literature has shown that under appropriate exposure to atmospheric CO_2, carbonation in slag-based geopolymers can drive the precipitation of natron ($Na_2CO_3 \cdot 10\,H_2O$), whereas nahcolite ($NaHCO_3$) prevails under accelerated carbonation conditions, and the formation of trona ($Na_3H(CO_3)_2 \cdot 2\,H_2O$) has been found to be higher with increases in temperature (Pouhet & Cyr, 2016; Bernal et al., 2012). The precipitation of such bicarbonates can notably decrease the pH (Bernal et al., 2012).

Cumulatively, the carbonation rate and susceptibility to carbonation of GPC are generally higher than PC concrete. Wasim et al. (2021) showed GPC to be more prone to carbonation than PC concrete after eight years of atmospheric exposure, with results showing greater steel corrosion levels within the GPC. Namely, the carbonation depth in GPC with 75:25 and 70:30 fly ash to GGBFS ratios ranged from 24 to 28 mm and 8–14 mm, respectively. Compared to PC concrete's carbonation depth (7–13 mm), the

first type of geopolymer exhibited much more degradation and the second type, a comparable level. It is worth noting that the first mixture contained additional Na_2SiO_3, which increased alkalinity and sorptivity. Further, it must be noted that the use of other testing procedures, such as the accelerated carbonation test, has been questioned by the literature (Shi et al., 2006; Pacheco-Torgal et al., 2015; Provis et al., 2015), with an indication that such tests over- estimate the carbonation levels of GPC. It has been argued that under normal atmospheric CO_2 levels (0.03–0.04%), the pore solution of AAMs can potentially sustain the pH at an adequate level to protect the steel reinforcement (Provis et al., 2015).

4.3. Resistance to sulfate attack

Deterioration from exposure to sulfate solutions can occur when concrete is in contact with groundwater and soils in arid regions or wastewater (Shi et al., 2006; Pacheco-Torgal et al., 2015). In PC concrete, the sulfates react with high-calcium systems, and the resultant products can cause internal stresses and deterioration. Due to the frequently lower calcium content of GPC, sulfate attack differs relative to PC concrete, particularly for exposures to sodium sulfate (Na_2SO_4) (Pacheco-Torgal et al., 2015; Provis et al., 2015). A study by Pacheco-Torgal et al. (2015) showed the exposure of GGBFS-based GPC and PC concrete in 5% (Na_2SO_4) and 5% $MgSO_4$ solutions for 12 months resulted in the (Na_2SO_4) solution contributing to 17% and 25% loss of compressive strength in GPC and PC concrete strength, respectively, and the $MgSO_4$ solution contributing to 23% and 37% reductions in the GPC and the PC concrete, respectively.

4.4. Resistance to acid attack

Literature shows that AAMs have superior resistance to acidic solutions compared to PC concrete (Nodehi & Taghvaee, 2022; Provis et al., 2015) because acidic solutions decalcify the high-calcium C-S-H system of PC concrete and dissolve $Ca(OH)_2$, leading

to deterioration. In the case of GPC, the acid attack produces the depolymerization of the aluminosilicate network structure and the formation of $Si(OH)_4$ (L. S. Wong, 2022). Yet, because AAMs typically contain little calcium, they have been shown to exhibit ~80% less acidic degradation than PC concrete (Nodehi & Taghvaee, 2022). Even in high-calcium AAMs, the acidic-induced corrosion is less impactful. For example, the investigation by Ariffin et al. (2013) comparing the mass loss and compressive strength degradation of POFA-based GPC and PC concrete showed that after 18 months of 2% sulfuric acid exposure, the mass loss of the GPC specimen was 8% less than the one observed in the PC concrete. Moreover, after the same period, the GPC exhibited a 35% reduction in compressive strength, whereas the PC concrete showed a 68% reduction.

4.5. Fire resistance

Studies have shown that GPC exhibits considerably higher resistance to elevated temperatures, such as fire, when compared to PC concrete (Nodehi & Taghvaee, 2022; Pacheco-Torgal et al., 2015) have claimed AAMs are suitable for passive fire protection applications under intermediate temperatures (< 900 °C) and can resist up to 1350 °C. For example, Shi et al. (2006) reported the development of geopolymer binders with resistance up to 1200 °C. In Shi et al.'s work, this desirable behavior was ascribed to the material's high endothermicity and to the nano-porosity of the tecto-aluminosilicate 3D networks of the composite that allowed physically and chemically bonded water to evaporate without causing any damage.

4.6. Alkali-silica reaction

The alkali-silica reaction is a chemical interaction between the hydroxyl ions of an alkaline system and siliceous constituents in the mixture, generally in the aggregates, that leads to internal stresses and cracking of concrete (Nodehi & Taghvaee, 2022). GPC typically contains high alkali contents, and the literature suggests that AAMs exhibit significant

amounts of this reaction product; nevertheless, in most cases, their expansion has been reported as less than PC concrete tested in parallel (Provis et al., 2015). Paudel et al. (2020) concluded that fly ash-based GPC is notably less vulnerable to alkali-silica reaction than PC concrete, as Fourier-transform infrared spectroscopy testing showed lower alkali-silica reaction gel formation in geopolymer mixtures at 365 days of age. The Fourier-transform infrared spectroscopy test demonstrated the formation of alkali-silica reaction gel in PC specimens at 803, 782 and 777 cm^{-1} wave numbers, whereas these peaks were not observed in the GPC samples. As with carbonation and chloride ingress, the aptness of the PC testing method for alkali-silica reaction, ASTM C1260, has been questioned for GPC (Pacheco-Torgal et al., 2015). Moreover, AAMs are often cured in different conditions than PC concrete to avoid the leaching of alkalis at early ages, making the procedure not directly compliant with the ASTM test method.

4.7. Resistance to freezing and thawing

Freezing and thawing cycles in cold climates can result in internal cracking and surface scaling (Pacheco-Torgal et al., 2015). Again, testing methods regularly used for PC concrete have been called into question as they are not representative of the actual service conditions (Pacheco-Torgal et al., 2015; Wasim et al., 2021). In addition, the activation of raw materials, such as fly ash, GGBFS, and metakaolin, seems to counteract the effect of frost attack and improve the strength of the GPC under testing, a condition that is not desirable. Consequently, authors such as Pacheco-Torgal et al. (2015) have recommended postponing the testing until the binder reactions in the AAMs are no longer affecting the microstructure of GPC. In examining GPC after these reactions are no longer causing notable changes to the microstructure, promising results for GPC are still attained. Aygörmez et al. (2020) investigated the durability of fly ash-based GPC after 365 days of casting. Interestingly, the authors found minor losses in the GPC strength after 300 freeze-thaw cycles, with a peak residual compressive strength of 41.5

MPa. Weight losses were observed to be very low as well, ranging between 0.24 and 0.88%.

Chapter 5

Reinforcing and Bonding

Reinforcing concrete helps contribute to tensile strength and ductility. Standard concrete reinforcement methods include embedding steel reinforcing bars (rebar) and adding fibers into the mixture. Properties such as bond strength between the reinforcement and concrete and corrosion are commonly of interest when implementing reinforced concrete (Institution of Civil Engineers, 2009). This section presents parameters driving the ability to use rebar in GPC (summarized in Table 5.1) and findings on the use of fiber reinforcement in GPC.

Table 5.1: Impact of GPC parameters on reinforcing and bonding.

GPC parameter	**Reinforcing**	**Bonding**
Alkaline activator	↕	↕
Precursor	↕	↕
Increasing the water content	↓	↓
Increasing the chemical admixtures content	↕	↕
Bar type	↕	↕
Increasing the bar diameter	↓	↓
Increasing the embedded length of reinforcing bars	↓	↓
Heat curing	↑	↑
Corrosion	↓	↓

Table based on Topark-Ngarm et al. (2015), Songpiriyakij et al. (2011), Al-Azzawi et al. (2018), Laskar and Talukdar (2017), Albidah et al. (2020), Maranan et al. (2015), Kim and Park (2014), Castel and Foster (2015), Albitar et al. (2017), Farhan et al. (2018).
↑ Indicates an improvement in the property.
↓ Indicates a deleterious effect on the property.
↕ Indicates improvement or deleterious impact on the property, depending on the mixture proportion.

5.1. Effect of the alkaline activator on reinforcing and bonding

While some alkali activators can improve bonding, beneficial effects are inconsistent across all activators. For example, in a study by Topark-Ngarm et al. (2015), the bond strength between rebar and high-calcium fly ash GPC and a blend of NaOH and Na_2SiO_3 activators, with 10 M, 15 M, and 20 M concentrations, increased with the concentration of NaOH solution, as did the compressive and tensile strengths. Similarly, Songpiriyakij et al. (2011) found that the compressive strength and bond strength between rebar and low-calcium fly ash GPC were superior with higher concentrations of NaOH, with specific findings suggesting the highest compressive and bonding strengths were with a 70% fly ash and 30% silica fume mixture activated with NaOH 18 M (see Figure 5.1a). However, Al-Azzawi et al. (2018) investigated the effect of the Na_2SiO_3/NaOH ratio for a Class-F fly ash GPC, but their results showed no clear trends relating to the effects on bond strength. Rather, findings from these authors suggested that differences in solid precursor characteristics would outweigh the effects of the Na_2SiO_3/NaOH ratio.

5.2. Effect of the solid precursor on reinforcing and bonding

There have been too few studies to robustly characterize individual drivers from solid precursors on bond strength, but as with other GPC properties, the bond strength can be tuned through an appropriate selection of solid precursors. Factors can be driven by the composition and morphology of the solid precursors as well as their interactions with the activators selected. For example, Laskar and Talukdar (2017) examined the effect of fly ash content on the bond strength between GPC made with ultra-fine GGBFS and showed a peak level of fly ash replacement beyond which there could be loss in bond strength, ∼30% fly ash. Similar findings were echoed in a study by Al-Azzawi et al. (2018), who also showed the characteristics of the fly ash itself could outweigh the effects of other mixture design decisions on bond strength. These authors ascribed the higher bond strength with the use of some fly ash as a function of mobility of the particles, small

particle size, high content of CaO, and, where present, a high proportion of SiO2 and Al2O3 in the fly ash.

Beyond fly ash, Songpiriyakij et al. (2011) studied the impact of rice husk bark ash and silica fume on fly ash-based GPC and bond strength with two different grades of rebar. These authors showed for both 10 M and 18 M concentrations of NaOH, the mixtures with the higher silica fume content exhibited higher bond strength. However, mixtures prepared with NaOH 10 M at 28 days possessed only 85% of the bond strength developed by the control PC concrete. In contrast, mixtures with NaOH 18 M and 10% or more silica fume had equivalent or greater bond strength to the PC concrete. Their findings suggest that rice husk bark and silica fume can partially replace fly ash in GPC and achieve adequate bonding, but only if the NaOH concentration is high.

5.3. Effect of the water content on reinforcing and bonding

It has been suggested that an increased water content lowers bond strength. A key example was presented by Al-Azzawi et al. (2018), who showed for their GPC blend, changing water content from ∼7 to ∼15 kg/m^3 yielded a maximum reduction of 38% in the bond strength.

5.4. Effects of chemical admixtures and additives on reinforcing and bonding

The level and type of admixtures used in GPC can influence the bond strength. For example, in a study by Laskar and Talukdar (2017), the role of SPs, namely sulfonated naphthalene-based SP and polycarboxylate ether-based SP, on the bonding between GPC made with ultra-fine GGBFS and rebar of size 16 mm diameter was examined. These authors showed an improvement in bond strength with low levels of SP, but segregation and low bond strength occurred in mixtures with more than 1.5% SP.

5.5. Effect of the rebar on reinforcing and bonding

While not a characteristic of the GPC, the rebar can also influence bond strength. Albidah et al. (2020) examined the use of hot rolled steel rebars and glass fiber-reinforced polymer (GFRP) bars, each 12 mm diameter, in metakaolin-based GPC. These authors observed that steel rebars presented 4% – 38% higher bond strength than GFRP bars (see Figure 5.1b).

Further, the reinforcing bar diameter will affect the bond strength between GPC and rebar (e.g., Maranan et al. (2015); Kim and Park (2014)). Maranan et al. (2015) showed the bond strength between fly ash and GGBFS-based GPC and GFRP bars lowers with increasing bar diameter. Kim and Park (2014) presented similar results for steel reinforcing bars, indicating that the bond strength between fly ash and GGBFS-based GPC and rebar decreases with the increase in the diameter of the reinforcing bars; they reported bond strengths of approximately 23 MPa, 18 MPa and 17 MPa for bar diameters of 10 mm, 16 mm and 25 mm, respectively (see Figure 5.1c). Furthermore, these authors found that these strengths were superior to that of PC with the same reinforcements. And it has been shown that bond strength can be improved in GPC concrete by leveraging rebar surface characteristics: Castel and Foster (2015) reported an increase of 10% in the bond strength between the GPC and ribbed bars at 28 days.

The embedded length of the rebar will also influence bond strengths. Maranan et al. (2015) studied the bond strength between fly ash and GGBFS-based GPC and GFRP bars. These authors showed that greater embedded lengths of the GFRP bars reduce the bond strength, regardless of the reinforcing bar diameter (see Figure 5.1d). Tekle et al. (2016) corroborate these results, showing a decrease in bond strength between fly ash-based GPC and longer embedded lengths of GFRP reinforcement bars.

5.6. Effect of curing conditions on reinforcing and bonding

As with compressive strength development, the curing temperature can influence the bond strength between GPC and reinforcement. Topark-Ngarm et al. (2015) reported the bond strength between rebar and high-calcium fly ash GPC with several alkali activator concentrations (NaOH 10 M, 15 M and 20 M) improved with the use of heat curing for 24 h at 60 ± 2 °C relative to room temperature curing at 23 ± 2 °C. Castel and Foster (2015) similarly showed for their low-calcium fly ash-based GPC, curing at 80 °C for 48 h was necessary to develop equal or improved bond strength with reinforcing steel bars compared to ordinary PC concrete.

5.7. Effect of corrosion on reinforcing and bonding

As would be expected, corrosion will further influence bond strength. While negligible effects on strength were noted by Albitar et al. (2017) with corrosion levels (CL) between 0 and 1%, a substantial loss in bond strength was reported for higher corrosion levels (1% $<$ CL $\leq$ 85%). Further, another experimental investigation was conducted by Farhan et al. (2018), which showed that the bond strength between reinforcing steel bars and steel fiber-reinforced GPC diminished due to corrosion. Notably, the samples reinforced with steel fibers presented less bond strength reduction than the plain GPC.

Bond strength assessment is critical for reinforced GPC, and the literature has studied several parameters influencing its behavior, as shown in Figure 5.1. The spectrum of bond strengths found in the literature ranges from ∼4 MPa to ∼25 MPa. Notably, there is a clear trend in the effect of increasing the reinforcement bar diameter, with a bond strength decrease of around 24 MPa (Figure 5.1c). The reinforcement bar diameters found in the literature range from 10 to 25 mm, and the embedded length of the reinforcement bars ranges from 5 to 15 times the diameter.

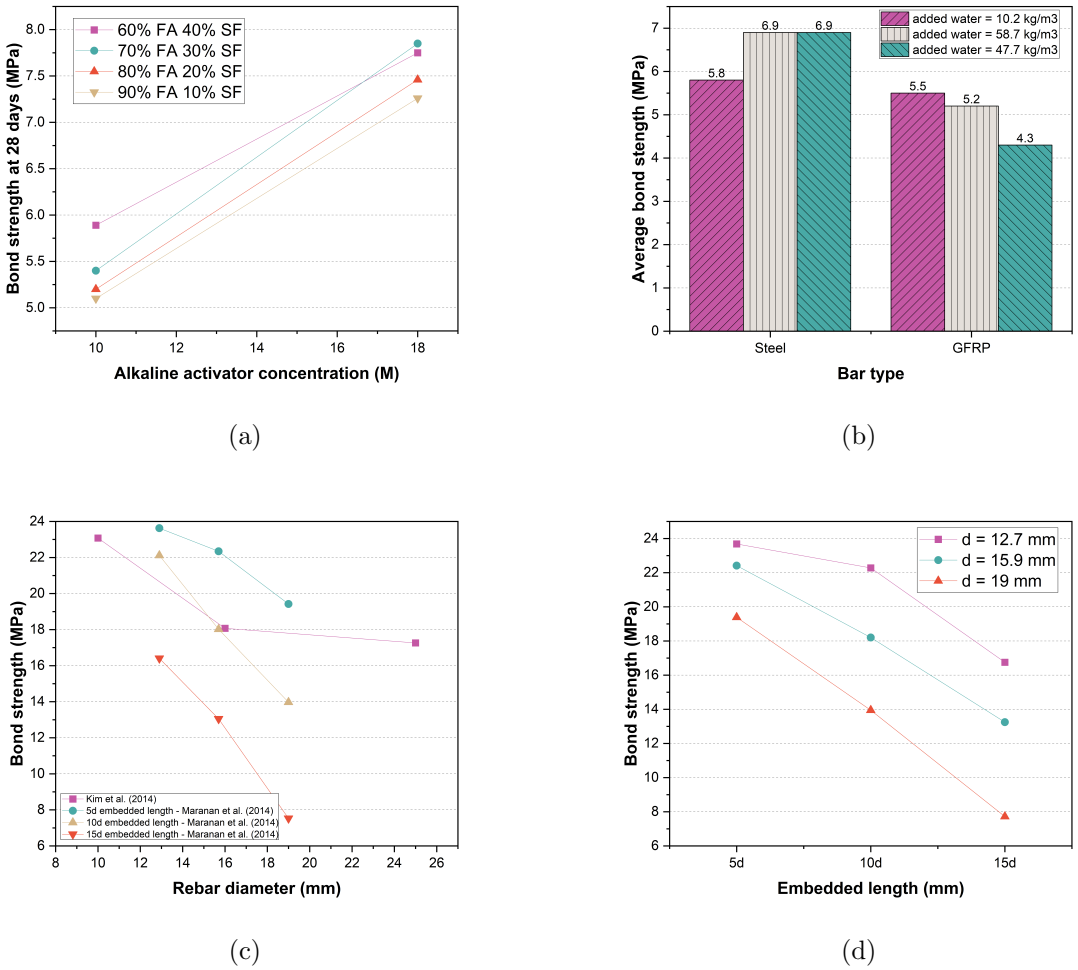

Figure 5.1: (a) Bond strength as a function of the alkaline activator concentration for different fly ash and silica fume proportions (Songpiriyakij et al., 2011), b) Bond strength comparison between two types of bar reinforcement in metakaolin-based GPC with different added water proportions (Albidah et al., 2020), c) Bond strength as a function of the rebar diameter for fly ash and GGBFS-based GPC (Maranan et al., 2015; Kim & Park, 2014), d) Bond strength as a function of embedded length with multiple diameters in fly ash and GGBFS-based GPC (Maranan et al., 2015).

5.8. Fiber reinforcing

Beyond rebar, the incorporation of fibers in GPC can be used to increase tensile strength and improve energy dissipation in fracture (Pacheco-Torgal et al., 2015). In Table 5.2, the literature on fiber-reinforced GPC is summarized, specifying the type of fiber and the properties assessed in each study.

Table 5.2: Summary of fiber-reinforced GPC properties studies.

Reference	Fiber type	Compressive strength	Splitting tensile strength	Flexural strength	Bond strength	Impact strength	Fracture toughness	Modulus of elasticity	Workability
Alomayri et al. (2013), Alomayri et al. (2014)	Cotton	-	-	x	-	x	x	-	-
Ganesh (2021)	Glass	x	x	x	-	x	-	-	x
Aisheh et al. (2022)	Steel	x	x	x	-	-	-	x	x
Wang et al. (2020)	Polypropylene	x	x	x	-	-	-	-	x
Noushini et al. (2018)	Synthetic (polymer)	x	x	x	-	-	x	x	-
Ma et al. (2019)	Micro-cable	-	-	x	x	-	-	-	-
Bakthavatchalam (2021)	Hybrid basalt/steel	x	x	x	-	-	-	-	x
Jia et al. (2020)	Graphene	-	-	x	-	-	x	x	-
	Carbon nanotube	-	-	x	-	-	x	x	-
	Graphite	-	-	x	-	-	-	-	-
	Aluminum oxide	-	-	x	-	-	x	x	-
	Chromium powder	-	-	x	-	-	-	-	-
	Fly-ash cenosphere	x	-	-	-	-	-	-	-
	Silicon dioxide	-	-	x	-	-	-	x	-
	Short carbon	-	-	x	-	-	x	x	-
	Short SiC	x	-	x	-	-	x	-	-
	Hybrid SiC/carbon	-	-	x	-	-	x	x	-
	Continuous	-	-	x	-	-	-	-	-

x Indicates an improvement in the property.
- Indicates a deleterious effect on the property.

Chapter 6

Code Committees and Standards for Construction with GPC

6.1. Code committees with adapting standards for GPC

Several standardizing bodies provide codes for cementitious materials testing and utilization. Due to the global adoption of codes from a few regions, this work focuses on the standardizing bodies within the United States, the European Union, and the United Kingdom. Eight leading organizations are responsible for the codes pertaining to cement in these regions.

- American Concrete Institute (ACI): the ACI is a United States-based non-profit organization that develops technical standards and resources for different concrete technologies. The codes developed by ACI are implemented in over 30 countries, resulting in them being used by over 30% of the world's population (Awad, 2017). At the time of this work, ACI has not created any standards concerning GPC, but there are suggestions in the ACI 318–19 building code to facilitate the implementation of alternative concrete, and other ACI committees have published reports dedicated to alternative cement (see Section 6.2).
- ASTM International: ASTM International is an organization that standardizes test methods for a broad spectrum of materials, including methods for assessing

PC. Many ASTM test specifications align with the chemical composition of PC concrete, but some performance-based test methods may apply to GPC (see Section 6.2).

- American Association of State Highway and Transportation Officials (AASHTO): AASHTO is a standard-setting organization (including cement-based materials standards) in the United States that promulgates road and highway design and construction provisions.
- International Organization for Standardization (ISO): ISO is a standard-setting body that develops technical and non-technical documents for various applications, including hydraulic cement test methods. The ISO 29581–1 (Cement – Test methods Part 1) (ISO 29581-1, 2009) and ISO 29581–2 (Cement – Test methods Part 2) (ISO 29581-2, 2010) can be directly applied to determine the loss on ignition, x–ray fluorescence spectrometry and wet chemistry methods of GPC (see Section 6.2).
- Eurocode 2: the European Standard EN 1992: "Design of concrete structures or Eurocode 2," is the governing code for structural applications in the European Union. It is formulated to measure and regulate concrete properties and performance, with no specific provisions for types of cementitious materials (concrete mixtures are covered in EN197–1, but GPC is not listed). Practitioners who adopt European codes must assess whether the current specifications can be applied to GPC through experimentation.
- fib Model Code 2020 (MC 2020): The Fédération International du Béton (fib) is a non-profit organization that provides codes for concrete structural design and sustainability, economic, and conservation considerations. The fib Model Code 2010 recognizes the importance of the performance-based approach – a characteristic that could better facilitate the use of alternative binders like AAMs – however, there are currently no guides for alternative cementitious materials, such as GPC.

- Institution of Civil Engineers (ICE): ICE is an association of civil engineering professionals in the United Kingdom that has developed an ICE Manual of Construction Materials, which acknowledges the advantages of GPC (Institution of Civil Engineers, 2009). However, they have not published any specifications regarding construction with GPC.
- British Standards Institution (BSI): The BSI is the United Kingdom's national standard-setting body. A member of the ISO, the BSI is a non-profit organization that develops standardized test methods to assess different materials and processes. They have created the BSI PAS 8820:2016 (British Standards Institution, 2016), one of the world's few performance-based standards dedicated to construction with alkali-activated materials (see Section 6.2).

While outside the regions of study, the authors note that Australia has recently adopted the code SA TS 199:2023 titled "Design of geopolymer and alkali-activated binder concrete structures," which will facilitate the utilization of geopolymers (Committee BD-002, 2016), and such codes can be adopted or adapted by other areas and support increased utilization of these materials.

6.2. Standards for construction with GPC

6.2.1. ACI standards and reports.

The ACI 318–19 standard regulates the use of structural concrete in a wide range of applications to ensure the protection of the public (ACI Committee 318, 2019), and it notes the potential utilization of materials such as GPC. While the ACI 318–19 code does not provide any fundamental specifications for alternative cement, a formal definition of alternative cement is given, and suggestions for their application are provided, including reference to technical reports from the organization, ACI ITG-10R-18 (ACI Innovation Task Group 10, 2018b) and ACI ITG-10.1R-18 (ACI Innovation Task Group 10, 2018a), to assess the applicability of alternative cement. The implementation of alternative building

materials that are not specifically contemplated in the code, such as GPC, is permitted upon authorization of the building official or a board of engineers designated by the building official (ACI Committee 318, 2019). The proof includes, but is not limited to, data and analysis of the material performance, test results, utilization requirements, and documentation of prior successful use (ACI Committee 318, 2019).

The ACI Innovation Task Group 10 developed the ACI ITG-10R-18 report to describe commercially available, emerging alternative cement and provide guidance for their utilization, including mix design, properties and characterization. This report covers clinkered alternative cement, calcinated alternative cement, and non-clinkered alternative cement (including AAMs), and it claims alkali-activated fly ash and alkali-activated slag cement can be used in the same applications of PC (ACI Innovation Task Group 10, 2018b).

Separately, the ACI Technical Committee 242 has developed a document for alkali-activated cement: the ACI PRC-242-22 report (ACI Committee 242, 2022), presenting information regarding design considerations, fresh-state properties, mechanical properties, durability, current challenges, and successful case studies. In this report, descriptions are also provided for mixture and curing considerations. Several material properties are explored in this report, including workability, setting time, hydration kinetics, compressive strength, modulus of elasticity, and creep of alkali-activated binders (ACI Committee 242, 2022). A discussion is provided for drivers of such performance characteristics.

6.2.2. Testing specifications.

Because GPC is still an emerging technology compared to PC concrete, there are not the same level of robust specifications for AAMs or GPC. As a result, practitioners regularly rely on existing PC and PC concrete specifications and assess their suitability with geopolymer binders and concrete. Tables 6.1 and 6.2 summarize the test methods found in ACI ITG-10.1R-18 (ACI Innovation Task Group 10, 2018a) for evaluating different

properties of PC and PC concrete and their suitability with GPC cement and GPC, respectively.

6.2.3. Testing specifications.

The BSI PAS 8820:2016 standard (United Kingdom) (British Standards Institution, 2016) provides definitions and performance-based provisions for AAMs and GPC made with aluminosilicate precursors and an activating solution. Notably, this specification does not prescribe the chemical composition of AAMs, giving flexibility to practitioners seeking to optimize their mixtures and implement alternative designs. This specification relies on the existing British standards for testing cement and concrete (e.g., BS EN 196, BS EN 197, BS EN 206, etc.), and it introduces modifications, limits, and performance requirements to evaluate AAMs properly. A complete list of the alkali-activated cementitious materials and alkali-activated concrete properties specified in BSI PAS 8820:2016 is presented in Table C.1.

6.2.4. Existing applications of alkali-activated materials in buildings.

There are several successful case studies of the implementation of GPC. These include the construction of the Global Change Institute at the University of Queensland, Australia, where PC was entirely replaced by alkali-activated fly ash and alkali-activated slag binder facilitated by the performance-based nature of the Australian Standard (ACI Innovation Task Group 10, 2018b). The Brisbane West Wellcamp Airport project provides another notable example of construction with AAMs, where a blend of alkali-activated fly ash and alkali-activated slag were employed to build one bridge and several pavements, curbs, road barriers, piles, pads, and median strips (ACI Innovation Task Group 10, 2018b).

Table 6.1: Summary of standards for PC and their suitability with AAMs and geopolymer binders. Table based on ISO 29581-1 (2009); ISO 29581-2 (2010); ACI Innovation Task Group 10 (2018a); ASTM C114 (2018); ASTM C1365 (2018); ASTM C204 (2018); ASTM C618 (2019); ASTM C109/C109M (2020); ASTM C151/C151M (2016); ASTM C1038/C138M (2019); ASTM C494/C494M (2019); ASTM C191 (2019); ASTM C186 - 15a (2015); ASTM C1702 - 15b (2015); ASTM C1698 (2014).

Test	Specification	Suitability with GPC	Notes
Loss on ignition (LOI)	ASTM C114 ISO 29581–1	Applicable*	• ASTM C114 does not establish optimal limits for alternative cement, although the tests could be directly applied. For calculating alternative cement's LOI, section 18.2 presents an applicable method for mixtures containing GGBFS. • The scope of ISO 29581-1 allows practitioners to use other methodologies and materials to demonstrate equivalence; therefore, wet chemistry analysis methods can be applied to geopolymer binders without specification constraints. • Discussion: Existing quantitative chemical analysis can capture the composition of alternative cement's constituents; however, specifying limits for these constituents is a notable challenge given the wide ranges observed in AAMs (see Table B.1). Establishing limits for individual cases hinders standardization, but broad limits can prevent the detection of harmful amounts of a particular component.
X-ray fluorescence spectrometry (XRS)	ASTM C114 ISO 29581–2	Applicable*	• See previous remarks on ASTM C114. • Like ISO 29581-1, this method applies to geopolymer binders due to the performance-based nature of its provisions. • Discussion: See notes in loss on ignition test.
X-ray diffraction (XRD)	ASTM C1365	Applicable*	• Although several phases are contemplated (e.g., alite, belite, aluminate, ferrite, calcite, etc.), the standard only addresses procedures and fails to provide any limits or ranges. XRD is directly applicable, but the appropriate specification is unspecified. • Discussion: see notes in loss on ignition test.

Continued on next page

Table 6.1 – continued from previous page

Test	Specification	Suitability with GPC	Notes
Thermogravimetric analysis or differential thermal analysis	ASTM C114	Applicable*	• See previous remarks on ASTM C114.
Wet chemistry methods	ASTM C114	Applicable*	• See previous remarks on ISO 29581-1.
Fineness	ASTM C204 ASTM C618	May be applicable***	• ASTM C204 provides a suitable instrument for PC (Blaine air-permeability apparatus); however, practitioners must determine whether this would work with cements of different characteristics. There are no rigorous prescriptions. • Table 2 of ASTM C618 limits the maximum percentage of particles retained in sieve No. 325 (45 µm) to 34% for all types of fly ash. • Discussion: The particle size of solid precursors and aggregates in AAMs strongly influences reactivity and strength. Therefore, reporting fineness should be a requirement in dedicated standards. Current test methods will likely work on the majority of AAM precursors (e.g., slag, metakaolin, silica fume); however, specific limits and optimum sizes depend on the precursor's nature and need to be determined on a case-by-case basis.
Density	ASTM C188	Applicable	• The density of alternative cements could be determined with current methods for PC, including the Le Chatelier Flask apparatus presented in ASTM C188-17. Other alternatives for measuring density, such as novel helium pycnometers devices, are available. • Discussion: There are existing test methods for measuring density that fit alternative binders. Performance-based standards might rely on such methods to report the mixture's density.

Continued on next page

Table 6.1 – continued from previous page

Test	Specification	Suitability with GPC	Notes
Compressive strength	ASTM C109/ C109M	Applicable**	• ASTM C109/C109M requires measuring the compressive strength at 24 hours, 3 days, 7 days, and 28 days and comparing the results with Table 2 of the standard. This comparison is problematic for geopolymers because 1) their optimal curing temperature can differ from that of PC, and 2) the 28-day measurement may not be an ideal age to examine their strength. • Discussion: Because compressive strength is paramount for all applications and because practitioners still need PC's performance as a reference, changing the ages of testing is challenging. On the other hand, these ages might put AAMs at a disadvantage if they exhibit fast strength development after certain age. A possible solution is to develop standards that categorize strength grades according to curing needs or verified strength gain rates.

Continued on next page

Table 6.1 – continued from previous page

Test	Specification	Suitability with GPC	Notes
Volume stability	ASTM C151/ C151M ASTM C1038 /C1038M	Applicable***	• In ASTM C151/C151M (autoclave expansion test), the temperature range in which the specimens are cast (216 ± 2 ℃) benefits geopolymer binders' curing; consequently, the method will likely be compatible with alternative binders. • ASTM C1038/C1038M could be applied to AAMs with sulfate excess; nonetheless, undesirable expansion could still occur after 14 days due to their alternative composition, making further examination advisable. • Discussion: Though the autoclave conditions benefit geopolymers, these materials could develop issues related to volume stability that are not tied to MgO and CaO hydration but rather prompted by their specific chemical composition. A case-by-case assessment would be more appropriate. ASTM C1038/C1038M provides a suitable method for detecting sulfate excess and subsequent instability, but the age of testing might not detect the expansive reactions catalyzed by other constituents. Dedicated test methods and specification limits for AAMs would facilitate their study, but again, the case-by-case requirements can hinder the establishment of such limits.

Continued on next page

Table 6.1 – continued from previous page

Test	Specification	Suitability with GPC	Notes
Setting time	ASTM C494 /C494M ASTM C191	May be applicable	• ASTM C494/C494M provisions exclude geopolymer binders and any other cementitious material that does not meet the Type I and Type II cement chemical composition. The primary concern for practitioners is that chemical admixtures might not provide the same benefits when applied to geopolymers. • ASTM C191 applies to alternative cement, but practitioners could find different needle penetration responses and other difficulties when establishing the mixing cycle and normal consistency if the rheology of the materials differs from PC. • Discussion: though noncompliant with the chemical composition dictated in ASTM C494/C494M, AAMs can still meet the requirements presented in Table 1 of the standard due to their highly tunable setting times. However, the viscosity induced by the alkaline activator and the variable effect of chemical admixtures on AAMs may pose some impracticalities. A similar conclusion can be drawn for ASTM C191 (Vicat needle test). Performance-based standards must consider these issues.

Continued on next page

Table 6.1 – continued from previous page

Test	Specification	Suitability with GPC	Notes
Heat of hydration	ASTM C186 ASTM C1702	Not applicable May be applicable	• The partial insolubility of specific components in acidic mediums and the water/cementitious material ratio requirement make ASTM C186 unsuitable for calculating alternative cement's heat of hydration. • Although ASTM C1702 is suitable for alternative cement testing, these materials' broad spectrum of composition and heat evolution restrict standardization. • Discussion: the unique chemical composition of AAMs is the major obstacle for standardizing the heat of hydration calculation (or heat of reaction, for AAMs that do not involve hydration). The isothermal conduction calorimetry test (ASTM C1702) offers a promising alternative to ASTM C186, but standardization is restricted given the broad spectrum of reaction kinetics in the early ages of myriad AAMs. Further, if a water/cementitious material ratio needs to be specified, this should be consistent with each mixture optimum parameters.
Admixture compatibility	ASTM C494 /C494M ASTM C1698	May be applicable	• See previous remarks on ASTM C494/C494M. • The ACI Task Group 10 recommends using ASTM C1698 to perform isothermal conduction calorimetry and assess the hydration kinetics between alternative cement and multiple admixtures. • Discussion: as noted with the case of SPs, chemical admixtures might prompt unexpected adverse effects on other properties when applied to improve workability (e.g., substantial loss in compressive strength). This directly compromises the compliance with ASTM C494/C494M performance limits. Careful consideration must be given to the admixture compatibility of AAMs when formulating dedicated standards.

* Without defined specification limits.
** Partially applicable in hydraulic cement, may not be suitable if not hydraulic.
*** Needs a case-by-case assessment.

Table 6.2: Summary of standards for PC concrete and their suitability with AAMs and GPC. Table based on ACI Innovation Task Group 10 (2018a); ASTM C39/C39M (2020); ASTM C78/C78M (2021); ASTM C293/C293M (2015); ASTM C496/C496M (2011); ASTM C469/469M (2022); ASTM C1399/C1399M (2015); ASTM C1550 (2020); ASTM C1609/C1609M (2019); AASTHO T 336-15 (2019); ASTM E119 (2020); ASTM C157/C157M (2017); ASTM A944 (2015); ASTM C666/C666M (2015); ASTM C1556 (2022); ASTM C1202 (2022); ASTM C150/C150M (2021); ASTM C1260 (2021); ASTM C1293 (2020); ASTM C1567 (2022).

Test	Specification	Suitability with GPC	Notes
Compressive strength	ASTM C39/ C39M	Applicable*	• This standard refers to ASTM C192/C192M to prescribe aggregates, mixing procedures, curing regime, and consolidation – likely leading to unoptimized properties for alternative concretes. • Discussion: Creating performance-based standard methods to measure and compare the compressive strength of GPC concretes would be incredibly beneficial. See discussion about compressive strength in Table 6.1.
Tensile strength	ASTM C78/ C78M ASTM C293/ C293M ASTM C496/ C496M	May be applicable	• ASTM C78/C78M, ASTM C293/C293M and ASTM C496/C496M rely on ASTM C192/C192M, which prescribes the chemical composition of the mixture and prevents direct compliance with the method for geopolymer binder concretes. Further, the required moist-curing regime is unsuitable with most alternative cements. • Discussion: The measurement of flexural strength using a simple beam with a third-point loading (ASTM C78) or a center-point loading (ASTM C293) has been applied to AAMs in the literature with modifications. This is because these standards prescribe mixing and curing, thus preventing direct compliance for most AAMs. Though the required moist curing method is suitable for some AAMs, it might be harmful to some others, leading to premature leaching and strength loss. Performance-based standards would benefit AAMs, but again, the broad spectrum of compositions and optimal curing regimes might restrict specifications.

Continued on next page

Table 6.2 – continued from previous page

Test	Specification	Suitability with GPC	Notes
Young's modulus and Poisson's ratio	ASTM C469/ C469M	Applicable	• Applying ASTM C469/469M to GPC is possible but questionable since it relies on the apparatus of ASTM C39/C39M and is therefore tied to the same constraints regarding alternative concretes posed by ASTM C192/C192M. • Discussion: See Notes regarding compressive strength in Table 6.2.
Ductility	ASTM C1399/ C1399M ASTM C1550 ASTM C1609/ C1609M	Not applicable Applicable Not applicable	• The applicability of ASTM C1399/C1399M in GPC is limited due to the prescription of mixing and moist-curing regime by ASTM C192, which is not necessarily optimal for GPC. • Since ASTM C1550 is not subjected to the prescription of ASTM C192 for mixture preparation, it is directly applicable to GPC. • ASTM C1609/C1609M is in accordance with ASTM C192; therefore, implementing GPC will not comply with this test method. • Discussion: The determination of toughness is crucial for fiber-reinforced specimens. AAMs can be directly assessed by the central point load mechanism presented in ASTM C1550, since it will not lead to issues associated with moist curing (see discussion about Tensile Strength). Other test methods might be applicable depending on the type of AAM and its response to moist curing.
Temperature effects	AASHTO 336 ASTM E119	Applicable	• AASHTO 336 can be directly applied to GPC, but since the coefficient of thermal expansion depends on mixture design, developing a test method for GPC that considers moisture conditions and specific composition would be ideal for GPC adoption. • ASTM E119 is suitable for evaluating both PC concrete and alternative concrete mixtures. • Discussion: Many AAMs showcase excellent thermal behavior, as noted in Section 5.5. Practitioners would benefit from the standardization of temperature effects measurements in AAMs; however, establishing harmonized mixing conditions might be challenging.

Continued on next page

Table 6.2 – continued from previous page

Test	Specification	Suitability with GPC	Notes
Shrinkage	ASTM C157/ 157M	Applicable	• Section 4.3 of ASTM C157/C157M allows practitioners to utilize alternative mixture designs and curing regimes; therefore, this test method is likely applicable to GPC concretes. • Discussion: Performance-based standards can rely on ASTM C157/C157M to determine the drying shrinkage of AAMs.
Bond strength	ASTM A944	Applicable	• ASTM A944 requires 1) a curing compound or plastic membrane to avoid rapid evaporation and 2) a concrete strength between 31 and 38 MPa at the moment of the test. Because this standard does not prescribe the concrete mixture design, GPC is included in its scope. • Discussion: Utilization of ASTM A944 is suitable for AAMs and GPC due to its performance-based nature. Both requirements can be satisfied by these alternative concrete mixtures.
Resistance to freezing-thawing	ASTM C666/ C666M	Applicable	• Though ASTM C666/C666M applies to GPC, the freezing-thawing resistance is better assessed in field tests. It is advisable to study the freezing-thawing resistance behavior of GPC carefully in conditions that resemble its potential application. • Discussion: As noted in Chapter 4, durability under freeze-thaw cycling might not be accurate if the testing conditions do not resemble the service conditions. Further, the activation of raw materials can offset frost attacks and improve the strength of AAMs. Therefore, age of testing should be postponed until geopolymerization dynamics no longer influence the microstructure of the specimen.

Continued on next page

Table 6.2 – continued from previous page

Test	Specification	Suitability with GPC	Notes
Resistance to fluid transport	ASTM C1556 ASTM C1202	Applicable May be applicable	• It is essential to highlight that geopolymer concrete has low permeability during the hardened stage, and the pore solution composition may influence the results of ASTM C1556. • ASTM C1202 might not be the most conclusive alternative for testing chloride resistance due to the unpredictability caused by the microstructural differences in GPC mixtures. • Discussion: Though applicable to AAMs and GPC, the complexities associated with the microstructure of these alternative concretes can result in inaccuracies. For example, the alkali activator can alter the pore chemistry and compromise the ASTM C1202 testing.
Resistance to sulfate attack	ASTM C1012/ C1012M	Not applicable	• Applying ASTM C1012/C1012M to predict the sulfate resistance of concretes with alternative chemical compositions may lead to erroneous results. • Discussion: For example, immersing an alkali-activated specimen in a sulfate solution to measure the change length may not be reflective of the appropriate deterioration mechanisms after several weeks if the mixture was previously synthesized with a sulfate-based activator.
Resistance to acids	**	**	**

Continued on next page

Table 6.2 – continued from previous page

Test	Specification	Suitability with GPC	Notes
Resistance to alkali-aggregate reaction	ASTM C1260 ASTM C1293 ASTM C1567	May be applicable	• Since ASTM C1260 is susceptible to changes in the mixture proportions, solution strengths, environmental conditions and cement composition, empirical correlations associated with the internal expansion of the concrete due to alkali reactions may not hold for alternative cement concretes. • ASTM C1293 could apply to GPC and other alternative concretes under the following conditions: 1) adjustment of the workability formulation and 2) addition of NaOH to increase the alkali content of the concrete. • Standard ASTM C1567 is subjected to the same limitations as ASTM C1260; therefore, developing dedicated standards for alternative binder concretes would be favorable. • Discussion: The resistance to alkali-aggregate reaction is a complex process to assess, especially when blends of myriad constituents are involved in synthesizing AAMs and the specimen needs to be subjected to specific environments. For example, ASTM C1260 requires a curing regime of 24 hours, which might not be optimal for certain AAMs, which are often cured in different conditions than PC concrete to avoid the leaching of alkalis at early ages. Standardizing the resistance to alkali-aggregate reaction in AAMs requires further modifications of existing standards (e.g., curing requirements, establishing alkaline activator limits).

* According to ACI Innovation Task Group 10 (2018a), its use is "questionable"; however, the test of failure under compressive load is valid.
** There are no existing tests to evaluate acid or chemical attack – ad hoc methodologies are employed (ACI Innovation Task Group 10, 2018a).

Chapter 7

Conclusions and Future Work

Geopolymer concrete (GPC) is a promising alternative to ordinary Portland cement (PC) due to its potential environmental benefits and tunable material performance. However, the wide range of mixture parameters that can be altered, their influence on material performance, and the complexity of the standardization process have resulted in limitations in implementation. This review highlights these issues to provide context for researchers and practitioners. Several key findings from this review are highlighted below:

- An increase in the alkaline activator liquid content, the water content, the Na_2SiO_3-to-NaOH activating solution ratio, and the use of superplasticizers and spherical-shaped aggregates enhance the workability of GPC. However, increasing the molarity of the alkaline activator solution, the aggregate-to-binder ratio, and the pigment content can lead to a less workable GPC. These parameters and the viscosity of GPC relative to PC concrete can also affect finishing and placement.
- The literature suggests compressive strength of GPC commonly increases with the concentration of NaOH in the alkaline activator, the content of GGBFS, the use of a good aggregate gradation, and, where appropriate, higher temperatures during the curing process. Reductions in compressive strength have been reported with higher water content and high pigment dosages. Adding superplasticizer to the mixtures influences strength, but not in a substantial amount.

Tensile and flexural strength follow similar trends, though the effect of certain parameters is more pronounced in some cases.

- The literature indicates that GPC can exhibit acceptable resistance to chloride ingress, sulfate attack, elevated temperatures, ASR and freeze and thawing, but it may be more prone to carbonation compared to PC concrete. It should be noted that many testing procedures used for measuring the durability of PC do not capture the GPC behavior accurately.
- Similar drivers for compressive strength also influence bond strength between GPC and rebar. Notably, rebar characteristics, including bar diameter and embedded length, also affect bond strength.
- There are no dedicated standards or codes for alternative cementitious materials in the United States and the European Union, resulting in the common application of PC specifications, which are not always well suited for GPC – often a function of the prescriptive nature of common standards and their not resulting in optimal AAM behavior. Thus, developing performance-based standards for alternative cementitious materials is needed in these regions.
- The United Kingdom, through the British Standards Institution (BSI), created one of the few dedicated standards for GPC, the BSI PAS 8820:2016 specification, which could lay the groundwork for other regions.

In future work, other factors that drive the implementation of AAMs and GPC should be considered to improve engineering understanding and to drive further adoption. These next steps of work should include further assessment of alternate resources for solid precursors and alkali- activators. Particularly, assessment of these materials should consider solid precursors that do not already have a market and alkali-activators that are not cost-prohibitive. Additionally, continued and improved development of standards and codes should be pursued, particularly the use of performance-based standards where applicable. Future analysis should robustly integrate quantitative environmental impact assessment into the valuation of resources used in GPC to determine benefits that could be accrued

through their systematic use. Additionally, techno-economic analyses of resources used and any variations in construction practice should be performed and integrated into material comparisons. Resource availability and localized burdens that could occur from selected materials or the application, use, and disposal of GPC should be considered. Cumulatively, these stages of analysis should demonstrate sustainable manufacturing, reduce environmental burdens (such as GHG emissions), and achieve competitive prices for GPC as an alternative to the established PC concrete.

Appendix A

Literature Review Methodology

This literature review leveraged academic and grey literature to provide context for codes, constructability, and material performance drivers that influence the implementation of geopolymer binders. Sources include reports from concrete-related institutions, standard test methods from standard-developing organizations, and peer-reviewed research articles and books. These searches were conducted from November 2022 to April 2023 through search engines: Google, Google Scholar, and Compass (ASTM International search engine), as well as the ACI, ICE, AASHTO, and ISO search engines. A total of 167 documents were collected for the review. The research methodology diagram is shown in Figure A.1 below.

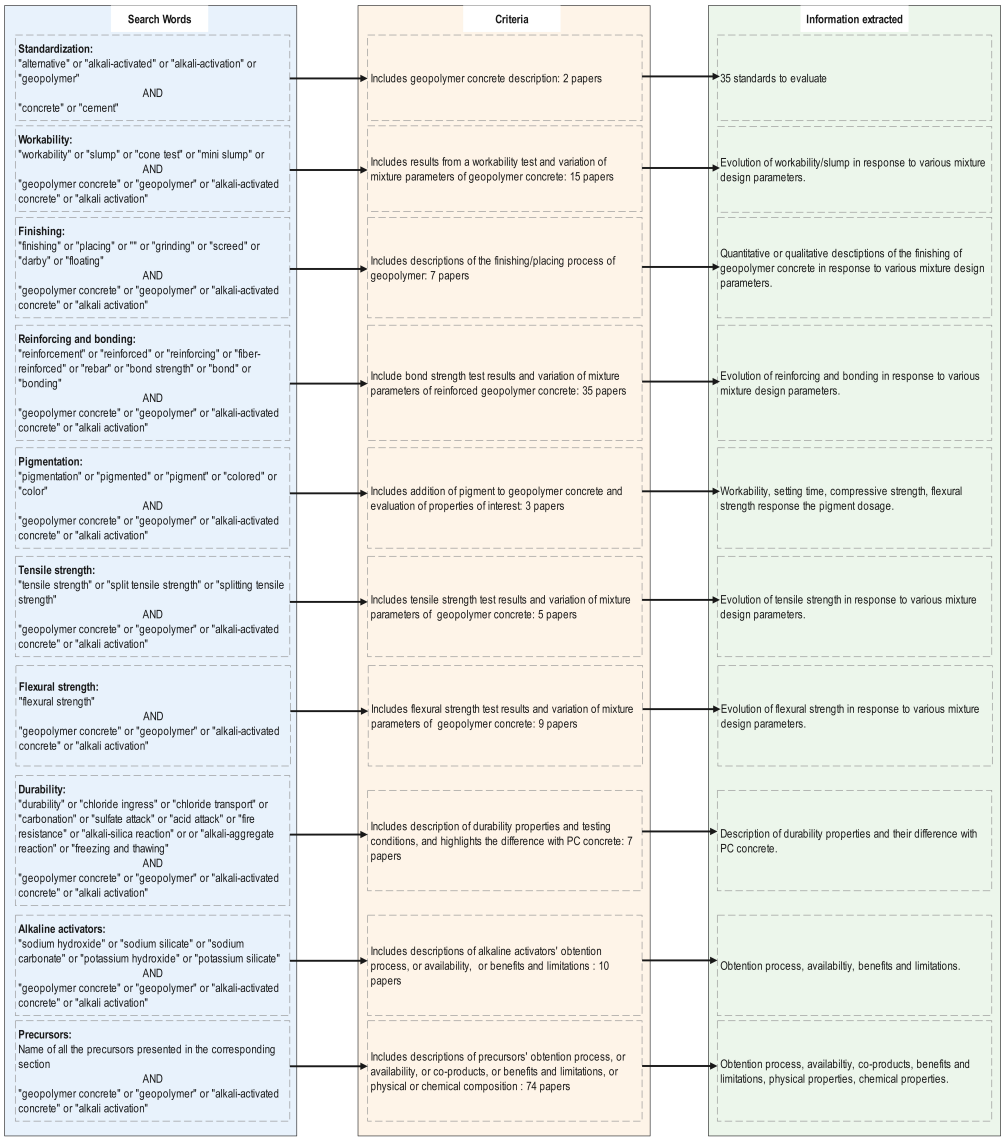

Figure A.1: Methodology diagram for the review.

Appendix B

Physical and Chemical Properties of Various Precursors and Alkaline Activators

Table B.1: Impact of GPC parameters on reinforcing and bonding. Table based on Nodehi and Taghvaee (2022); García-Lodeiro et al. (2015); Ding and Li (2002); Almutairi et al. (2021); Cordeiro et al. (2011); J. He et al. (2013); Liu et al. (2014); Tran et al. (2019); Sprynskyy et al. (2010); Alcantara et al. (2000); of Encylopaedia Britannica (2018); Dobiszewska (2020); Hyndman and Drury (1977); Villar-Cociña et al. (2011); Onikeku et al. (2019); Pereira et al. (2021); Thomas et al. (2021); El-Sayed and El-Samni (2006); Al-Akhras et al. (2009); Tangchirapat et al. (2012); Chandra et al. (2019); Kroehong et al. (2011); Yang et al. (2023); Trishna (n.d.); Navarro et al. (2017); Marsh et al. (2021); N. Wong et al. (2022); Wang et al. (2021); Mehdizadeh et al. (2018); Maghsoodloorad and Allahverdi (2016).

Aluminosilicate precursor	**Specific surface area** (m^2/kg)	**Specific gravity**	**Bulk density** (kg/m^3)	**Average particle size (µm)**	**Shape**	**Color**
FA	250-500	2.1-3.0	540-860	0.5-300	Spherical	Grey, dark grey
GGBFS	400-600	2.9	1000-1300	125-250	Angular	Off-white
MK	120000	2.23	890	1-20	Angular	White
SF	15000-30000	2.2-2.3	130-430 (undensified) 480-720 (densified)	0.15	Spherical	Black, dark grey
RHA	30000-80000	2.3	550-700	1-20	Irregular	Grey, black
RM	11650-30720	3.94	2700-3200	0.8-50	Irregular, needle-shaped	Red
WG	-	-	1800	-	Angular	Colorless
NZ (Clinoptilolite)	13400 (air dried)	2.34	1650	45-1000 (grounded)	Crystalline, microporous	Colorless; red, brown or pink (with impurities)
BA	350	2.99	2795	20	Angular	Dark-colored or light-colored

Continued on next page

Table B.1 – continued from previous page

Alumino-silicate precursor	**Specific surface area** (m^2/kg)	**Specific gravity**	**Bulk density** (kg/m^3)	**Average particle size (µm)**	**Shape**	**Color**
BLA	35000-500000	2.25-2.8	365 (loose) 479 (rodded)	17-58	Irregular	Grey
RSA	1846	2.1-2.25	400-700	3.3	Irregular	Grey
OWA	410	2.13	500-800	10	Irregular	Grey
POFA	670-1490	1.7-2.5	780-1120	2.1-15.6	Irregular	Black, dark grey
MT (Kaolinite)	10000-20000	2.6	2630	2	Irregular	White, gray
SiMnS	450-600	2.9-3.2	2800	9.5	Irregular	Light yellow, light green
GPS	300-400	2.94	1600-1800	10-100	Angular	Black, dark grey

Table B.2: Chemical composition of selected aluminosilicate precursors. Table based on García-Lodeiro et al. (2015); Albidah et al. (2020); Miller et al. (2019); J. He et al. (2013); Tran et al. (2019); Mao et al. (2022); Thomas et al. (2021); Tangchirapat et al. (2012); Qaidi et al. (2022); Navarro et al. (2017); Wang et al. (2021).

Alumino-silicate precursor	**Silicon dioxide (SiO_2)**	**Aluminum oxide (Al_2O_3)**	**Titanium oxide (TiO_2)**	**Ferric oxide (Fe_2O_3)**	**Calcium oxide (CaO)**	**Magnesium oxide (MgO)**	**Sodium oxide (Na_2O)**	**Potassium oxide (K_2O)**	**Phosphorus oxide (P_2O_5)**	**Sulphur trioxide (SO_3)**
Class-F FA	42.6-59.8	21.8-34.5	-	6.3-18.1	2.8-7.0	1.2-2.6	0.15-0.94	0.38-6.0	-	0.19-1.9
Class-C FA	34.1	14.2	-	7.2	38	1.5	0.44	1.4	-	4.2
GGBFS	27-40	5-33	< 3	< 1	30-50	1-2.1	1-3	1-3	0.02-0.09	< 3
MK	51.0	42.6	1.71	2.11	1.29	0.13	0.28	0.34	0.05	0.44
SF	90	0.40	-	0.40	1.60	-	0.50	2.2	-	0.40
RHA	88.51	0.28	0.02	0.44	1.03	0.47	0.33	2.60	0.63	0.49
RM	1.2	14.0	4.5	30.9	2.5	-	-	-	-	-
NZ (Clinoptilolite)	62.8	12.3	-	0.08	4.34	1.05	0.26	0.94	-	-
BA	53.38	17.95	-	10.72	6.48	6.38	-	-	-	-
BLA	78.71	1.01	0.08	0.54	7.82	1.83	0.05	3.78	0.99	1.0
RSA	79.82	1.13	-	0.245	0.37	7.54	0.501	1.07	3.75	-
OWA	11.70	2.51	0.11	1.26	10.20	3.03	-	42.66	2.97	3.60
POFA	55.5	9.2	-	5.6	12.4	4.6	-	-	-	2.3
MT (Kaolinite)	72.55	16.44	-	1.90	0.05	0.83	0.08	3.06	-	-
SiMnS	36.53	9.86	0.19	0.92	29.10	4.69	0.34	1.08	0.35	2.77
GPS	41.8	4.6	0.32	1.74	45.3	1.26	-	0.47	3.48	-

Table B.3: Physical properties of selected alkaline activators. Table based on Bordwell (1988); US Environmental Protection Agency (2007); Wikipedia (2023c, 2023d, 2023b, 2023e, 2023a).

Alkaline activator	**State**	**Density (g/cm^3) at 25 °C**	**Melting point (°C)**	**Solubility in water (g/cm^3) at 25 °C**	**Alkalinity (pKb)**	**Color**	**Odor**
NaOH	Liquid (common state for alkali activation), powder, crystals, pellets, flakes, compounder, beads.	2.13	323	1	0.2	Colorless (liquid), white (solid)	Odorless
Na_2SiO_3	Liquid (common state for alkali activation), powder, crystals, pellets.	2.61	1088	0.22	4.2	Colorless (liquid), white (solid).	Odorless
Na_2CO_3	Liquid, powder (common state for alkali activation), crystals.	2.54	851	0.307	3.7	Colorless (liquid), gray/white (powder).	Odorless
KOH	Liquid, powder (common state for alkali activation), pellets, flakes.	2.12	360	1.21	0.5	Colorless (liquid), white (powder).	Odorless
K_2SiO_3	Liquid, solid (common state for alkali activation).	1.24	760	< 0.000336	3.3	Colorless (liquid), white (solid).	Odorless
Na_2SO_4	Liquid, solid, powder (common state for alkali activation), crystals, pellets.	2.66	884	0.28	3.67	Colorless (liquid), white (powder)	Odorless

Appendix C

British Standards Institution Specifications

Table C.1: Properties of alkali-activated cementitious material (AACM) and alkali-activated concrete (AAC) specified in BSI PAS 8820:2016 standard (British Standards Institution, 2016).

AACM properties specified in BSI PAS 8820:2016	**AAC properties specified in BSI PAS 8820:2016**
• Compressive strength (2, 7, and 28 days) by strength class • Initial setting time • Soundness (expansion) • Heat of reaction • Chloride content	• Admixtures • Aggregates • Other constituents (e.g., fibers and pigments) • Test schedule • Mixing, placement and curing • Slump (workability) • Compactability • Flow value • Compressive strength • Flexural strength • Tensile strength • Density • Durability • Drying shrinkage • Alkali-silica reaction • Freeze-thaw • Sulfate resistance • Carbonation • Chloride ingress

References

AASTHO T 336-15. (2019). Standard method of test for coefficient of thermal expansion of hydraulic cement concrete. *American Association of State Highway and Transportation Officials*.

ACI Committee 242. (2022). *Aci prc-242-22: Alkali-activated cements – report.* Retrieved from www.concrete.org

ACI Committee 318. (2019). *Aci 318-19 building code requirements for structural concrete and commentary*. American Concrete Institute. doi: 10.14359/51716937

ACI Innovation Task Group 10. (2018a). *Aci itg-10.1r-18: Report on alternative cements* (ACI ITG-10.1R-18 ed.). American Concrete Institute.

ACI Innovation Task Group 10. (2018b). *Aci itg-10r-18: Practitioner's guide for alternative cements* (ACI ITG-10R-18 ed.). American Concrete Institute.

Adesina, A. (2021). Performance and sustainability overview of sodium carbonate activated slag materials cured at ambient temperature. *Resources, Environment and Sustainability*, *3*, 100016. doi: 10.1016/j.resenv.2021.100016

Aisheh, Y. I. A., Atrushi, D. S., Akeed, M. H., Qaidi, S., & Tayeh, B. A. (2022, 12). Influence of polypropylene and steel fibers on the mechanical properties of ultra-high-performance fiber-reinforced geopolymer concrete. *Case Studies in Construction Materials*, *17*. doi: 10.1016/j.cscm.2022.e01234

Al-Akhras, N. M., Al-akhras, K. M., & Attom, M. F. (2009). Performance of olive waste ash concrete exposed to elevated temperatures. *Fire safety journal*, *44*, 370-375. doi: 10.1016/j.firesaf.2008.08.006

Al-Azzawi, M., Yu, T., & Hadi, M. N. (2018, 6). Factors affecting the bond strength between the fly ash-based geopolymer concrete and steel reinforcement. *Structures*, *14*, 262-272. doi: 10.1016/j.istruc.2018.03.010

Albidah, A., Altheeb, A., Alrshoudi, F., Abadel, A., Abbas, H., & Al-Salloum, Y. (2020, 10). Bond performance of gfrp and steel rebars embedded in metakaolin based geopolymer concrete. *Structures*, *27*, 1582-1593. doi: 10.1016/j.istruc.2020.07.048

Albitar, M., Visintin, P., Ali, M. S. M., Lavigne, O., & Gamboa, E. (2017, 1). Bond slip models for uncorroded and corroded steel reinforcement in class-f fly ash geopolymer concrete. *Journal of Materials in Civil Engineering*, *29*. doi: 10.1061/(asce)mt.1943-5533.0001713

Alcantara, E., Cheeseman, C., Knight, J., & Loizidou, M. (2000). Properties of alkali-activated clinoptilolite. *Cement and Concrete Research*, *30*, 1641-1646.

Aliabdo, A. A., Abd Elmoaty, M., & Salem, H. A. (2016). Effect of water addition, plasticizer and alkaline solution constitution on fly ash based geopolymer concrete performance. *Construction and Building Materials*, *121*, 694–703.

Al-Majidi, M., Lampropoulos, A., & Cundy, A. B. (2016). Effect of alkaline activator, water, superplasticizer and slag contents on the compressive strength and workability of slag-fly ash based geopolymer mortar cured under ambient temperature. *International Journal of Civil, Environmental, Structural, Construction and Architectural Engineering*.

Almutairi, A. L., Tayeh, B. A., Adesina, A., Isleem, H. F., & Zeyad, A. M. (2021, 12). Potential applications of geopolymer concrete in construction: A review. *Case Studies in Construction Materials*, *15*. doi: 10.1016/j.cscm.2021.e00733

Alomayri, T., Shaikh, F. U., & Low, I. M. (2013, 7). Characterisation of cotton fibre-reinforced geopolymer composites. *Composites Part B: Engineering*, *50*, 1-6. doi: 10.1016/j.compositesb.2013.01.013

Alomayri, T., Shaikh, F. U., & Low, I. M. (2014, 4). Synthesis and mechanical properties of cotton fabric reinforced geopolymer composites. *Composites Part B: Engineering*, *60*, 36-42. doi: 10.1016/j.compositesb.2013.12.036

Alzeebaree, R., Çevik, A., Mohammedameen, A., Niş, A., & Gülşan, M. E. (2020). Mechanical performance of frp-confined geopolymer concrete under seawater attack. *Advances in Structural Engineering*, *23*(6), 1055–1073.

Andrews-Phaedonos, F. (2011). *Geopolymer "green" concrete-reducing the carbon footprint-the vicroads experience.*

Ariffin, M. A., Bhutta, M. A., Hussin, M. W., Tahir, M. M., & Aziah, N. (2013). Sulfuric acid resistance of blended ash geopolymer concrete. *Construction and Building Materials*, *43*, 80-86. doi: 10.1016/j.conbuildmat.2013.01.018

Asha, P., Salman, A., & Kumar, R. A. (2014). Experimental study on concrete with bamboo leaf ash. *International Journal of Engineering and Advanced Technology (IJEAT)*, 2249-8958.

Assi, L. N., Carter, K., Deaver, E., & Ziehl, P. (2020). Review of availability of source materials for geopolymer/sustainable concrete. *Journal of Cleaner Production*, *263*, 121477. doi: 10.1016/j.jclepro.2020.121477

ASTM A944. (2015). Standard test method for comparing bond strength of steel reinforcing bars to concrete using beam-end specimens. *ASTM International*. Retrieved from www.astm.org doi: 10.1520/A0944-10R15

ASTM C1038/C138M. (2019). Standard test method for expansion of hydraulic cement mortar bars stored in water. *ASTM International*. Retrieved from www.astm.org doi: 10.1520/C1038_C1038M-19

ASTM C109/C109M. (2020). Standard test method for compressive strength of hydraulic cement mortars (using 2-in. or [50-mm] cube specimens). *ASTM International*. Retrieved from www.astm.org doi: 10.1520/C0109_C0109M-20

ASTM C114. (2018). Standard test methods for chemical analysis of hydraulic cement. *ASTM International*. Retrieved from www.astm.org doi: 10.1520/C0114-18

ASTM C1202. (2022). Standard test method for electrical indication of concrete's ability to resist chloride ion penetration. *ASTM International*. Retrieved from www.astm.org doi: 10.1520/C1202-22E01

ASTM C1260. (2021). Standard test method for potential alkali reactivity of aggregates (mortar-bar method). *ASTM International*. Retrieved from www.astm.org doi: 10.1520/C1260-21

ASTM C1293. (2020). Standard test method for determination of length change of concrete due to alkali-silica reaction. *ASTM International*. Retrieved from www.astm.org doi: 10.1520/C1293-20A

ASTM C1365. (2018). Standard test method for determination of the proportion of phases in portland cement and portland-cement clinker using x-ray powder diffraction analysis. *ASTM International*. Retrieved from www.astm.org doi: 10.1520/C1365-18

ASTM C1399/C1399M. (2015). Standard test method for obtaining average residual-strength of fiber-reinforced concrete. *ASTM International*. Retrieved from www.astm.org doi: 10.1520/C1399_C1399M-10R15

ASTM C150/C150M. (2021). Standard specification for portland cement. *ASTM International*. Retrieved from www.astm.org doi: 10.1520/C0150_C0150M-22

ASTM C151/C151M. (2016). Standard test method for autoclave expansion of hydraulic cement. *ASTM International*. Retrieved from www.astm.org doi: 10.1520/C0151_C0151M-16

ASTM C1550. (2020). Standard test method for flexural toughness of fiber reinforced concrete (using centrally loaded round panel) 1. *ASTM International*. Retrieved from www.astm.org doi: 10.1520/C1550-20

ASTM C1556. (2022). Standard test method for determining the apparent chloride diffusion coefficient of cementitious mixtures by bulk diffusion. *ASTM International*. Retrieved from www.astm.org doi: 10.1520/C1556-22

ASTM C1567. (2022). Standard test method for determining the potential alkali-silica reactivity of combinations of cementitious materials and aggregate (accelerated mortar-bar method). *ASTM International*. Retrieved from www.astm.org doi: 10.1520/C1567-22

ASTM C157/C157M. (2017). Standard test method for length change of hardened hydraulic-cement mortar and concrete. *ASTM International*. Retrieved from www.astm.org doi: 10.1520/C0157_C0157M-17

ASTM C1609/C1609M. (2019). Standard test method for flexural performance of fiber-reinforced concrete (using beam with third-point loading). *ASTM International*. Retrieved from www.astm.org doi: 10.1520/C1609_C1609M-19A

ASTM C1698. (2014). Standard test method for autogenous strain of cement paste and mortar. *ASTM International*. Retrieved from www.astm.org doi: 10.1520/C1698-09R14

ASTM C1702 - 15b. (2015). Standard test method for measurement of heat of hydration of hydraulic cementitious materials using isothermal conduction calorimetry. *ASTM International*. Retrieved from www.astm.org doi: 10.1520/C1702-15B

ASTM C186 - 15a. (2015). Standard test method for heat of hydration of hydraulic cement. *ASTM International*.

ASTM C191. (2019). Standard test methods for time of setting of hydraulic cement by vicat needle. *ASTM International*. Retrieved from www.astm.org doi: 10.1520/C0191-19

ASTM C204. (2018). Standard test methods for fineness of hydraulic cement by air-permeability apparatus. *ASTM International*. Retrieved from www.astm.org doi: 10.1520/C0204-18

ASTM C293/C293M. (2015). Standardtest method for flexural strength of concrete (using simple beam with center-point loading) 1. *ASTM International*. Retrieved from www.astm.org doi: 10.1520/C0293_C0293M-15

ASTM C39/C39M. (2020). Standard test method for compressive strength of cylindrical concrete specimens. *ASTM International*. Retrieved from www.astm.org doi: 10.1520/C0039_C0039M-20

ASTM C469/469M. (2022). Standard test method for static modulus of elasticity and poisson's ratio of concrete in compression. *ASTM International*. Retrieved from www.astm.org doi: 10.1520/C0469_C0469M-22

ASTM C494/C494M. (2019). Standard specification for chemical admixtures for concrete. *ASTM International*. Retrieved from www.astm.org doi: 10.1520/C0494_C0494M

-19
ASTM C496/C496M. (2011). Standard test method for splitting tensile strength of cylindrical concrete specimens. *ASTM International*. Retrieved from www.astm.org doi: 10.1520/C0496_C0496M-11
ASTM C618. (2019). Standard specification for coal fly ash and raw or calcined natural pozzolan for use in concrete. *ASTM International*. Retrieved from www.astm.org doi: 10.1520/C0618-19
ASTM C666/C666M. (2015). Standard test method for resistance of concrete to rapid freezing and thawing. *ASTM International*. Retrieved from www.astm.org doi: 10.1520/C0666_C0666M-15
ASTM C78/C78M. (2021). Standard test method for flexural strength of concrete (using simple beam with third-point loading). *ASTM International*. Retrieved from www.astm.org doi: 10.1520/C0078_C0078M-21
ASTM E119. (2020). Standard test methods for fire tests of building construction and materials. *ASTM International*. Retrieved from www.astm.org doi: 10.1520/E0119-20
Awad, K. (2017). *Aci and the world.* Retrieved from https://www.concrete.org/news/newsdetail.aspx?f=51700829
Aygörmez, Y., Canpolat, O., & Al-Mashhadani, M. M. (2020). Assessment of geopolymer composites durability at one year age. *Journal of Building Engineering*, *32*, 101453.
Bakthavatchalam, K. (2021). An experimental investigation on potassium activator based geopolymer concrete incorporated with hybrid fibers. In (Vol. 46, p. 8494-8501). Elsevier Ltd. doi: 10.1016/j.matpr.2021.03.506
Bellum, R. R., Al Khazaleh, M., Pilla, R. K., Choudhary, S., & Venkatesh, C. (2022). Effect of slag on strength, durability and microstructural characteristics of fly ash-based geopolymer concrete. *Journal of Building Pathology and Rehabilitation*, *7*(1), 25.
Bernal, S. A., Provis, J. L., Brice, D. G., Kilcullen, A., Duxson, P., & Deventer, J. S. V. (2012, 10). Accelerated carbonation testing of alkali-activated binders significantly underestimates service life: The role of pore solution chemistry. *Cement and Concrete Research*, *42*, 1317-1326. doi: 10.1016/j.cemconres.2012.07.002
Blengini, G. A., Busto, M., Fantoni, M., & Fino, D. (2012). Eco-efficient waste glass recycling: Integrated waste management and green product development through lca. *Waste Management*, *32*, 1000-1008. doi: 10.1016/j.wasman.2011.10.018
Bligh, R., & Glasby, T. (2013). *Development of geopolymer precast floor panels for the global change institute at university of queensland.*
Bondar, D., Ma, Q., Soutsos, M., Basheer, M., Provis, J. L., & Nanukuttan, S. (2018, 11). Alkali activated slag concretes designed for a desired slump, strength and chloride diffusivity. *Construction and Building Materials*, *190*, 191-199. doi: 10.1016/j.conbuildmat.2018.09.124
Bordwell. (1988). *Bordwell pka table.*
British Standards Institution. (2016). *Bsi pas 8820-2016: Alkali-activated cementitious material and concrete – specification.*
Busch, P., Kendall, A., Murphy, C. W., & Miller, S. A. (2022, 7). *Literature review on policies to mitigate ghg emissions for cement and concrete* (Vol. 182). Elsevier B.V. doi: 10.1016/j.resconrec.2022.106278

Castel, A., & Foster, S. J. (2015). Bond strength between blended slag and class f fly ash geopolymer concrete with steel reinforcement. *Cement and Concrete Research*, *72*, 48-53. doi: 10.1016/j.cemconres.2015.02.016

Chandra, S., Mbewe, P. B. K., Kong, S. Y., & Savija, B. (2019). Agricultural solid waste as source of supplementary cementitious materials in developing countries. *Materials*. doi: 10.3390/ma12071112

Cherian, E., Kalavathy, G., Joshi, T. J., Phoebe, M. G. L., & Gurunathan, B. (2022). *Importance of nanocatalyst and its role in biofuel production.* Elsevier Inc. doi: 10.1016/B978-0-323-85269-2.00022-8

Committee BD-002. (2016). Sa ts 199 - 2023: design of geopolymer and alkali-activated binder concrete structures. *Australian Technical Specifications*.

Cordeiro, G. C., Filho, R. D. T., Tavares, L. M., Fairbairn, E. D. M. R., & Hempel, S. (2011). Influence of particle size and specific surface area on the pozzolanic activity of residual rice husk ash. *Cement and Concrete Composites*, *33*, 529-534. doi: 10.1016/j.cemconcomp.2011.02.005

Danish, A., Ozbakkaloglu, T., Mosaberpanah, M. A., Salim, M. U., Bayram, M., Yeon, J. H., & Jafar, K. (2022). Sustainability benefits and commercialization challenges and strategies of geopolymer concrete: A review. *Journal of Building Engineering*, *58*, 105005. doi: 10.1016/j.jobe.2022.105005

Ding, J. T., & Li, Z. (2002). Effects of metakaolin and silica fume on properties of concrete. *ACI Materials Journal*, *99*, 393-398. doi: 10.14359/12222

Dobiszewska, M. (2020). Physical properties and microstructure of concrete withwaste basalt powder addition. *Materials*, *13*. doi: 10.3390/MA13163503

El-Sayed, M. A., & El-Samni, T. M. (2006). Physical and chemical properties of rice straw ash and its effect on the cement paste produced from different cement types. *Journal of King Saud University Engineering Sciences*, *19*, 21-29. doi: 10.1016/S1018-3639(18)30845-6

Farhan, N. A., Sheikh, M. N., & Hadi, M. N. (2018). Experimental investigation on the effect of corrosion on the bond between reinforcing steel bars and fibre reinforced geopolymer concrete. *Structures*, *14*, 251–261.

Firdous, R., & Stephan, D. (2019, 9). Effect of silica modulus on the geopolymerization activity of natural pozzolans. *Construction and Building Materials*, *219*, 31-43. doi: 10.1016/j.conbuildmat.2019.05.161

Ganesh, A. C. (2021, 2). Development of high performance sustainable optimized fiber reinforced geopolymer concrete and prediction of compressive strength. *Journal of Cleaner Production*, *282*. doi: 10.1016/j.jclepro.2020.124543

García-Lodeiro, I., Palomo, A., & Fernández-Jiménez, A. (2015). Crucial insights on the mix design of alkali-activated cement-based binders. In F. Pacheco-Torgal, J. Labrincha, C. Leonelli, A. Palomo, & P. Chindaprasirt (Eds.), . Woodhead Publishing Series in Civil and Structural Engineering.

Ghadban, R. A. R., & Abdulrehman, M. A. (2022, 1). Study of some properties of colored geopolymer concrete consisting of slag. *Journal of the Mechanical Behavior of Materials*, *31*, 656-662. doi: 10.1515/jmbm-2022-0066

Ghafoor, M. T., Khan, Q. S., Qazi, A. U., Sheikh, M. N., & Hadi, M. N. (2021, 3). Influence of alkaline activators on the mechanical properties of fly ash based geopolymer concrete cured at ambient temperature. *Construction and Building Materials*, *273*.

doi: 10.1016/j.conbuildmat.2020.121752

Habert, G., Miller, S. A., John, V. M., Provis, J. L., Favier, A., Horvath, A., & Scrivener, K. L. (2020, 11). *Environmental impacts and decarbonization strategies in the cement and concrete industries* (Vol. 1). Springer Nature. doi: 10.1038/s43017-020-0093-3

Hameed, M. M., & Ali, A. M. (2021, 12). Using of metakaolin to produce colored geopolymer concrete. In (Vol. 2114). IOP Publishing Ltd. doi: 10.1088/1742-6596/2114/1/012018

Hassan, A., Arif, M., & Shariq, M. (2019a). Effect of curing condition on the mechanical properties of fly ash-based geopolymer concrete. *SN Applied Sciences*, *1*, 1–9.

Hassan, A., Arif, M., & Shariq, M. (2019b, 6). *Use of geopolymer concrete for a cleaner and sustainable environment – a review of mechanical properties and microstructure* (Vol. 223). Elsevier Ltd. doi: 10.1016/j.jclepro.2019.03.051

He, J., Jie, Y., Zhang, J., Yu, Y., & Zhang, G. (2013). Synthesis and characterization of red mud and rice husk ash-based geopolymer composites. *Cement and Concrete Composites*, *37*, 108-118. doi: 10.1016/j.cemconcomp.2012.11.010

He, X., Yuhua, Z., Qaidi, S., Isleem, H. F., Zaid, O., Althoey, F., & Ahmad, J. (2022). Mine tailings-based geopolymers: A comprehensive review. *Ceramics International*, *48*, 24192-24212. doi: 10.1016/j.ceramint.2022.05.345

Henigal, A. M., Sherif, M. A., & Hassan, H. H. (2017, 4). Study on properties of self-compacting geopolymer concrete. *IOSR Journal of Mechanical and Civil Engineering*, *14*, 52-66. doi: 10.9790/1684-1402075266

Hyndman, R., & Drury, M. (1977). *Physical properties of basalts, gabbros, and ultramafic rocks from dsdp leg 37.* Retrieved from http://journal.um-surabaya.ac.id/index.php/JKM/article/view/2203

Institution of Civil Engineers. (2009). *Ice manual of construction materials* (1st ed., Vol. 1; M. Forde, Ed.).

ISO 29581-1. (2009). *Iso 29581-1: Cement – test methods – part 1: Analysis by wet chemistry.*

ISO 29581-2. (2010). *Cement – test methods – part 2: Chemical analysis by x-ray fluorescence.*

Jia, D., He, P., Wang, M., & Yan, S. (2020). *Geopolymer and geopolymer matrix composites.* Springer Series in Materials Science.

Kapur, A., Keoleian, G., Kendall, A., & Kesler, S. E. (2008). Dynamic modeling of in-use cement stocks in the united states. *Journal of Industrial Ecology*, *12*, 539-556. doi: 10.1111/j.1530-9290.2008.00055.x

Khankhaje, E., Hussin, M. W., Mirza, J., Rafieizonooz, M., Salim, M. R., Siong, H. C., & Warid, M. N. M. (2016). On blended cement and geopolymer concretes containing palm oil fuel ash. *Materials and Design*, *89*, 385-398. doi: 10.1016/j.matdes.2015.09.140

Kim, J. S., & Park, J. H. (2014). An experimental evaluation of development length of reinforcements embedded ingeopolymer concrete. In (Vol. 578-579, p. 441-444). Trans Tech Publications Ltd. doi: 10.4028/www.scientific.net/AMM.578-579.441

Kroehong, W., Sinsiri, T., Jaturapitakkul, C., & Chindaprasirt, P. (2011). Effect of palm oil fuel ash fineness on the microstructure of blended cement paste. *Construction and Building Materials*, *25*, 4095-4104. doi: 10.1016/j.conbuildmat.2011.04.062

Kuenzel, C., Vandeperre, L. J., Donatello, S., Boccaccini, A. R., & Cheeseman, C. (2012). Ambient temperature drying shrinkage and cracking in metakaolin-based geopolymers. *Journal of the American Ceramic Society*, *95*(10), 3270–3277.

Kumar, A., Saravanan, T. J., Bisht, K., & Kabeer, K. I. A. (2021). A review on the utilization of red mud for the production of geopolymer and alkali activated concrete. *Construction and Building Materials*, *302*, 124170. doi: 10.1016/j.conbuildmat.2021.124170

Kwasny, J., Soutsos, M. N., McIntosh, J. A., & Cleland, D. J. (2018, 10). Comparison of the effect of mix proportion parameters on behaviour of geopolymer and portland cement mortars. *Construction and Building Materials*, *187*, 635-651. doi: 10.1016/j.conbuildmat.2018.07.165

Laskar, S. M., & Talukdar, S. (2017, 11). Preparation and tests for workability, compressive and bond strength of ultra-fine slag based geopolymer as concrete repairing agent. *Construction and Building Materials*, *154*, 176-190. doi: 10.1016/j.conbuildmat.2017.07.187

Liu, W., Chen, X., Li, W., Yu, Y., & Yan, K. (2014). Environmental assessment, management and utilization of red mud in china. *Journal of Cleaner Production*, *84*, 606-610. doi: 10.1016/j.jclepro.2014.06.080

Lokuge, W., Wilson, A., Gunasekara, C., Law, D. W., & Setunge, S. (2018). Design of fly ash geopolymer concrete mix proportions using multivariate adaptive regression spline model. *Construction and Building Materials*, *166*, 472–481.

Lv, Q., Yu, J., Ji, F., Gu, L., Chen, Y., & Shan, X. (2021, 5). Mechanical property and microstructure of fly ash-based geopolymer activated by sodium silicate. *KSCE Journal of Civil Engineering*, *25*, 1765-1777. doi: 10.1007/s12205-021-0025-x

Ma, G., Li, Z., Wang, L., & Bai, G. (2019, 1). Micro-cable reinforced geopolymer composite for extrusion-based 3d printing. *Materials Letters*, *235*, 144-147. doi: 10.1016/j.matlet.2018.09.159

Maghsoodloorad, H., & Allahverdi, A. (2016). Efflorescence formation and control in alkali-activated phosphorus slag cement. *International Journal of Civil Engineering*, *14*, 425-438. doi: 10.1007/s40999-016-0027-0

Mahmud, M. H., & Abdulrehman, M. A. (2021, 9). Studying some of the mechanical and physical properties of colored geopolymer concrete. *Journal of Engineering and Sustainable Development*, *25*, 2-49-2-59. doi: 10.31272/jeasd.conf.2.2.7

Mao, Q., Li, Y., Liu, K., Peng, H., & Shi, X. (2022). Mechanism, characterization and factors of reaction between basalt and alkali: Exploratory investigation for potential application in geopolymer concrete. *Cement and Concrete Composites*, *130*, 104526. doi: 10.1016/j.cemconcomp.2022.104526

Maranan, G., Manalo, A., Karunasena, K., & Benmokrane, B. (2015, 1). Bond stress-slip behavior: Case of gfrp bars in geopolymer concrete. *Journal of Materials in Civil Engineering*, *27*. doi: 10.1061/(asce)mt.1943-5533.0001046

Marsh, A., Yang, T., Adu-Amankwah, S., & Bernal, S. (2021). *Utilization of metallurgical wastes as raw materials for manufacturing alkali-activated cements*. Elsevier Ltd. doi: 10.1016/b978-0-12-820549-5.00009-7

Mather, B., & Ozyildirim, C. (2002). *Sp-1(02): Concrete primer*. ACI.

Mehdizadeh, H., Kani, E. N., Sanchez, A. P., & Fernandez-Jimenez, A. (2018). Rheology of activated phosphorus slag with lime and alkaline salts. *Cement and Concrete*

Research, *113*, 121-129. doi: 10.1016/j.cemconres.2018.07.010

Mermerdaş, K., Manguri, S., Nassani, D. E., & Oleiwi, S. M. (2017). Effect of aggregate properties on the mechanical and absorption characteristics of geopolymer mortar. *Engineering Science and Technology, an International Journal*, *20*, 1642-1652. doi: 10.1016/j.jestch.2017.11.009

Miller, S. A., Cunningham, P. R., & Harvey, J. T. (2019). Rice-based ash in concrete: A review of past work and potential environmental sustainability. *Resources, Conservation and Recycling*, *146*, 416-430. doi: 10.1016/j.resconrec.2019.03.041

Miller, S. A., & Myers, R. J. (2019). Environmental impacts of alternative cement binders. *Environmental science & technology*, *54*(2), 677–686.

Monteiro, P. J., Miller, S. A., & Horvath, A. (2017, 12). Towards sustainable concrete. *Nature Materials*, *16*, 698-699.

Montes, C., & Allouche, E. N. (2012, 1). Evaluation of the potential of geopolymer mortar in the rehabilitation of buried infrastructure. *Structure and Infrastructure Engineering*, *8*, 89-98. doi: 10.1080/15732470903329314

Nath, P., & Sarker, P. (2014, 9). Effect of ggbfs on setting, workability and early strength properties of fly ash geopolymer concrete cured in ambient condition. *Construction and Building Materials*, *66*, 163-171. doi: 10.1016/j.conbuildmat.2014.05.080

Nath, P., & Sarker, P. K. (2017, 1). Flexural strength and elastic modulus of ambient-cured blended low-calcium fly ash geopolymer concrete. *Construction and Building Materials*, *130*, 22-31. doi: 10.1016/j.conbuildmat.2016.11.034

Nath, S. K., Randhawa, N. S., & Kumar, S. (2022). A review on characteristics of silico-manganese slag and its utilization into construction materials. *Resources, Conservation and Recycling*, *176*, 105946. doi: 10.1016/j.resconrec.2021.105946

Navarro, R., Zornoza, E., Garcés, P., Sánchez, I., & Alcocel, E. G. (2017). Optimization of the alkali activation conditions of ground granulated simn slag. *Construction and Building Materials*, *150*, 781-791. doi: 10.1016/j.conbuildmat.2017.06.064

Nematollahi, B., & Sanjayan, J. (2014). Effect of different superplasticizers and activator combinations on workability and strength of fly ash based geopolymer. *Materials and Design*, *57*, 667-672. doi: 10.1016/j.matdes.2014.01.064

Nguyen, T. T., Goodier, C. I., & Austin, S. A. (2020, 11). Factors affecting the slump and strength development of geopolymer concrete. *Construction and Building Materials*, *261*. doi: 10.1016/j.conbuildmat.2020.119945

Nodehi, M., & Taghvaee, V. M. (2022). Alkali-activated materials and geopolymer: a review of common precursors and activators addressing circular economy. *Circular Economy and Sustainability*, *2*, 165-196. doi: 10.1007/s43615-021-00029-w

Noushini, A., Hastings, M., Castel, A., & Aslani, F. (2018, 10). Mechanical and flexural performance of synthetic fibre reinforced geopolymer concrete. *Construction and Building Materials*, *186*, 454-475. doi: 10.1016/j.conbuildmat.2018.07.110

Nuaklong, P., Sata, V., & Chindaprasirt, P. (2016). Influence of recycled aggregate on fly ash geopolymer concrete properties. *Journal of Cleaner Production*, *112*, 2300-2307. doi: 10.1016/j.jclepro.2015.10.109

Nuruddin, M. F., Demie, S., Ahmed, M. F., & Shafiq, N. (2011). Effect of superplasticizer and naoh molarity on workability, compressive strength and microstructure properties of self-compacting geopolymer concrete. *International Journal of Civil and Environmental Engineering*.

Nutakki, S. K., Reddy, V. S., Rao, M. V. S., & Shrihari, S. (2021). Effect of various parameters on the workability and strength properties of geopolymer concrete. *E3S Web of Conferences*, *309*, 01102. doi: 10.1051/e3sconf/202130901102

of Encylopaedia Britannica, T. E. (2018). Clinoptilolite. In (https://ww ed.).

Olsson, J. A., Miller, S. A., & Alexander, M. G. (2023). Near-term pathways for decarbonizing global concrete production. *Nature Communications*, *14*(1), 4574.

Onikeku, O., Shitote, S. M., Mwero, J., & Adedeji, A. A. (2019). The open construction & building evaluation of characteristics of concrete mixed with bamboo leaf ash. *The Open Construction & Building Technology Journal*, 67-80. doi: 10.2174/1874836801913010067

Pacheco-Torgal, F., Labrincha, J., Leonelli, C., Palomo, A., & Chindaprasirt, P. (2015). *Handbook of alkali-activated cements, mortars and concretes*. Woodhead Publishing Series in Civil and Structural Engineering.

Paudel, S. R., Yang, M., & Gao, Z. (2020). ph level of pore solution in alkali-activated fly-ash geopolymer concrete and its effect on asr of aggregates with different silicate contents. *Journal of Materials in Civil Engineering*, *32*(9), 04020257.

Pereira, L., Tamashiro, J., Guedes, F., Santos, L. D., Teixeira, S., Kinoshita, A., & Antunes, P. (2021). Bamboo leaf ash for use as mineral addition with portland cement. *Journal of Building Engineering*, *42*, 1-9. doi: 10.1016/j.jobe.2021.102769

Pouhet, R., & Cyr, M. (2016). Carbonation in the pore solution of metakaolin-based geopolymer. *Cement and Concrete Research*, *88*, 227–235.

Provis, J. L. (2018, 12). *Alkali-activated materials* (Vol. 114). Elsevier Ltd. doi: 10.1016/j.cemconres.2017.02.009

Provis, J. L., Palomo, A., & Shi, C. (2015). Advances in understanding alkali-activated materials. *Cement and Concrete Research*, *78*, 110-125. doi: 10.1016/j.cemconres.2015.04.013

Qaidi, S. M., Tayeh, B. A., Zeyad, A. M., de Azevedo, A. R., Ahmed, H. U., & Emad, W. (2022). Recycling of mine tailings for the geopolymers production: A systematic review. *Case Studies in Construction Materials*, *16*, e00933. doi: 10.1016/j.cscm.2022.e00933

Santhosh, K. G., Subhani, S. M., & Bahurudeen, A. (2022). Recycling of palm oil fuel ash and rice husk ash in the cleaner production of concrete. *Journal of Cleaner Production*, *354*, 131736. doi: 10.1016/j.jclepro.2022.131736

Scanferla, P., Gharzouni, A., Texier-Mandoki, N., Bourbon, X., & Rossignol, S. (2022). Effects of potassium-silicate, sands and carbonates concentrations on metakaolin-based geopolymers for high-temperature applications. *Open Ceramics*, *10*, 100257. doi: 10.1016/j.oceram.2022.100257

Shah, I. H., Miller, S. A., Jiang, D., & Myers, R. J. (2022). Cement substitution with secondary materials can reduce annual global co2 emissions by up to 1.3 gigatons. *Nature Communications*, *13*, 1-11. doi: 10.1038/s41467-022-33289-7

Shehata, N., Mohamed, O. A., Sayed, E. T., Abdelkareem, M. A., & Olabi, A. G. (2022). Geopolymer concrete as green building materials: Recent applications, sustainable development and circular economy potentials. *Science of the Total Environment*, *836*, 155577. doi: 10.1016/j.scitotenv.2022.155577

Shi, C., Krivenko, P., & Roy, D. (2006). *Alkali-activated cements and concretes*. Taylor and Francis.

Songpiriyakij, S., Pulngern, T., Pungpremtrakul, P., & Jaturapitakkul, C. (2011, 5). Anchorage of steel bars in concrete by geopolymer paste. *Materials and Design*, *32*, 3021-3028. doi: 10.1016/j.matdes.2011.01.048

Souza, A., Lima, D., Andrade, M., Oliveira, A., & Leonardo, H. (2023). Rigorous environmental and energy life cycle assessment of blast furnace pig iron in brazil: The role of carbon and iron sources , and co-product utilization. *Sustainable Materials and Technologies*, *36*. doi: 10.1016/j.susmat.2023.e00607

Sprynskyy, M., Golembiewski, R., Trykowski, G., & Buszewski, B. (2010). Heterogeneity and hierarchy of clinoptilolite porosity. *Journal of Physics and Chemistry of Solids*, *71*, 1269-1277. doi: 10.1016/j.jpcs.2010.05.006

Sreenivasulu, C., Jawahar, J. G., Reddy, M. V. S., & Kumar, D. P. (2015). Effect of fine aggregate blending on short-term mechanical properties of geopolymer concrete. *ASIAN JOURNAL OF CIVIL ENGINEERING (BHRC)*, *17*.

Suresh, D., & Nagaraju, K. (2015). Ground granulated blast slag (ggbs) in concrete – a review. *IOSR Journal of Mechanical and Civil Engineering*, *12*, 76-82.

Swilling, M., Hajer, M., Baynes, T., Bergesen, J., Labbé, F., Musango, J., ... Tabory, S. (2018). The weight of cities: Resource requirements of future urbanization. *International Resource Panel, United Nations Environment Programme*.

Tangchirapat, W., Khamklai, S., & Jaturapitakkul, C. (2012). Use of ground palm oil fuel ash to improve strength, sulfate resistance, and water permeability of concrete containing high amount of recycled concrete aggregates. *Materials and Design*, *41*, 150-157. doi: 10.1016/j.matdes.2012.04.054

Tayeh, B. A., Zeyad, A. M., Agwa, I. S., & Amin, M. (2021, 12). Effect of elevated temperatures on mechanical properties of lightweight geopolymer concrete. *Case Studies in Construction Materials*, *15*. doi: 10.1016/j.cscm.2021.e00673

Tekle, B. H., Khennane, . A., & Kayali, O. (2016). Bond properties of sand-coated gfrp bars with fly ash-based geopolymer concrete. *Journal of Composites for Construction*. doi: 10.1061/(ASCE)CC

Tempest, B., Snell, C., Gentry, T., Trejo, M., & Isherwood, K. (2015). *Manufacture of full-scale geopolymer cement concrete components: A case study to highlight opportunities and challenges.*

Tennakoon, C., Nicolas, R. S., Sanjayan, J. G., & Shayan, A. (2016, 12). Thermal effects of activators on the setting time and rate of workability loss of geopolymers. *Ceramics International*, *42*, 19257-19268. doi: 10.1016/j.ceramint.2016.09.092

Thomas, B. S., Yang, J., Bahurudeen, A., Chinnu, S. N., Abdalla, J. A., Hawileh, R. A., & Hamada, H. M. (2022, 3). *Geopolymer concrete incorporating recycled aggregates: A comprehensive review* (Vol. 3). Elsevier Ltd. doi: 10.1016/j.clema.2022.100056

Thomas, B. S., Yang, J., Mo, K. H., Abdalla, J. A., Hawileh, R. A., & Ariyachandra, E. (2021). Biomass ashes from agricultural wastes as supplementary cementitious materials or aggregate replacement in cement/geopolymer concrete: A comprehensive review. *Journal of Building Engineering*, *40*, 102332. doi: 10.1016/j.jobe.2021.102332

Topark-Ngarm, P., Chindaprasirt, P., & Sata, V. (2015, 7). Setting time, strength, and bond of high-calcium fly ash geopolymer concrete. *Journal of Materials in Civil Engineering*, *27*. doi: 10.1061/(asce)mt.1943-5533.0001157

Tran, Y. T., Lee, J., Kumar, P., Kim, K. H., & Lee, S. S. (2019). Natural zeolite and

its application in concrete composite production. *Composites Part B: Engineering*, *165*, 354-364. doi: 10.1016/j.compositesb.2018.12.084

Trishna, B. (n.d.). *Kaolinite: Structure, morphology and use — soil minerals.* Retrieved from https://www.soilmanagementindia.com/soil-mineralogy-2/kaolinite-structure-morphology-and-use-soil-minerals/13266

Triwulan, M., Ekaputri, J. J., & Priyanka, N. F. (2017). *The effect of temperature curing on geopolymer concrete.*

US Environmental Protection Agency. (2007). *Biopesticides registration action document - potassium silicate.*

Verma, M., & Dev, N. (2021). Sodium hydroxide effect on the mechanical properties of flyash-slag based geopolymer concrete. *Structural Concrete*, *22*, E368–E379.

Verma, M., & Dev, N. (2022a). Effect of ground granulated blast furnace slag and fly ash ratio and the curing conditions on the mechanical properties of geopolymer concrete. *Structural concrete*, *23*(4), 2015–2029.

Verma, M., & Dev, N. (2022b). Effect of snf-based superplasticizer on physical, mechanical and thermal properties of the geopolymer concrete. *Silicon*, *14*(3), 965–975.

Villar-Cociña, E., Valencia, E., Santos, S. F., Savastano, H., & Frías, M. (2011). Cement & concrete composites pozzolanic behavior of bamboo leaf ash: Characterization and determination of the kinetic parameters. *Cement and Concrete Composites*, *33*, 68-73. doi: 10.1016/j.cemconcomp.2010.09.003

Vincevica-Gaile, Z., Teppand, T., Kriipsalu, M., Krievans, M., Jani, Y., Klavins, M., ... Tamm (2021). Towards sustainable soil stabilization in peatlands: Secondary raw materials as an alternative. *Sustainability*, *13*(12), 6726.

Wang, Y., Aslani, F., & Valizadeh, A. (2020, 10). An investigation into the mechanical behaviour of fibre-reinforced geopolymer concrete incorporating niti shape memory alloy, steel and polypropylene fibres. *Construction and Building Materials*, *259*. doi: 10.1016/j.conbuildmat.2020.119765

Wang, Y., Xiao, R., Hu, W., Jiang, X., Zhang, X., & Huang, B. (2021). Effect of granulated phosphorus slag on physical, mechanical and microstructural characteristics of class f fly ash based geopolymer. *Construction and Building Materials*, *291*, 123287. doi: 10.1016/j.conbuildmat.2021.123287

Waqas, R. M., Butt, F., Zhu, X., Jiang, T., & Tufail, R. F. (2021, 9). A comprehensive study on the factors affecting the workability and mechanical properties of ambient cured fly ash and slag based geopolymer concrete. *Applied Sciences (Switzerland)*, *11*. doi: 10.3390/app11188722

Wasim, M., Ngo, T. D., & Law, D. (2021, 7). *A state-of-the-art review on the durability of geopolymer concrete for sustainable structures and infrastructure* (Vol. 291). Elsevier Ltd. doi: 10.1016/j.conbuildmat.2021.123381

Wikipedia. (2023a). *Potassium hydroxide.* Retrieved from https://en.wikipedia.org/wiki/Potassium_hydroxide

Wikipedia. (2023b). *Sodium carbonate.* Retrieved from https://en.wikipedia.org/wiki/Sodium_carbonate

Wikipedia. (2023c). *Sodium hydroxide.* Retrieved from https://en.wikipedia.org/wiki/Sodium_hydroxide

Wikipedia. (2023d). *Sodium metasilicate.* Retrieved from https://en.wikipedia.org/wiki/Sodium_metasilicate

Wikipedia. (2023e). *Sodium sulfate.* Retrieved from https://en.wikipedia.org/wiki/Sodium_sulfate

Wong, L. S. (2022, 3). *Durability performance of geopolymer concrete: A review* (Vol. 14). MDPI. doi: 10.3390/polym14050868

Wong, N., Siung, C. C., Chai, C., Khoso, A. R., Bamgbade, J., & Sambo, R. (2022). Physicochemical characteristics of silico manganese slag as a recycling construction material : A systematic review. *Research Square*, 1-22. doi: https://doi.org/10.21203/rs.3.rs-1667883/v1

Xie, J., Wang, J., Rao, R., Wang, C., & Fang, C. (2019, 5). Effects of combined usage of ggbs and fly ash on workability and mechanical properties of alkali activated geopolymer concrete with recycled aggregate. *Composites Part B: Engineering*, *164*, 179-190. doi: 10.1016/j.compositesb.2018.11.067

Yang, Y., Jaber, M., Michot, L. J., Rigaud, B., Walter, P., Laporte, L., ... Liu, Q. (2023). Analysis of the microstructure and morphology of disordered kaolinite based on the particle size distribution. *Applied Clay Science*, *232*, 106801. doi: 10.1016/j.clay.2022.106801